

1 **Lacustrine carbonate platforms; facies, cycles and tectono-sedimentary models for**
2 **the pre-salt Lagoa Feia Group (Early Cretaceous), Campos Basin, Brazil**

3 ¹ M. C. Muniz & ² D. W.J. Bosence

4 ¹ Petrobras, Av. Republica do Chile, 330 -17th Floor, ZIP:20.031.170 – Rio de Janeiro, Brazil

5 ² Department Earth Sciences, Royal Holloway University of London, Egham, Surrey, TW20 0EX, UK

6 *Corresponding author (mcalazans@petrobras.com.br)

7

8 **ACKNOWLEDGMENTS**

9 We thank Petrobras for providing the subsurface data and cores from the Southern
10 Campos Basin, for the permission to publish this work and for the sponsorship. We thank
11 Reviewers Sylvia Anjos and Joyce Neilson for their comments on our manuscript, and the
12 advice of AAPG Editors Katz and Scherrer are acknowledged for assistance in knocking
13 the paper into shape for the Bulletin.

14 **ABSTRACT**

15 Studies of lacustrine carbonate rocks in continental rifts have received a huge interest in
16 recent years because of their great economic value in the south Atlantic. However, most
17 existing facies and tectono-sedimentary models for carbonate platforms are based on
18 marine carbonate systems, whereas models for non-marine systems are scarce.

19 The main aim of this paper is the establishment of such models to further our
20 understanding of the late syn-rift Lower Cretaceous carbonate successions of the southern
21 Campos Basin, Brazil. This paper is based on a proximal to distal industrial dataset of 3-D
22 seismic, cores and well logs from the hydrocarbon producing Coqueiros Formation
23 (Coquina), Campos Basin. The dominant carbonate facies in the Coqueiros Formation are
24 mollusk-rich grainstones, rudstones and floatstones, which form the main reservoir facies.

25 3D seismic interpretations show an oblique extensional rift system, characterized by a
26 series of grabens, half-grabens, accommodation zones and horsts oriented NE-SW to
27 NNW-SSW. Three tectonic domains are recognized based on structural style, stretching

28 factors, subsidence rates as well as facies and different types of lacustrine carbonate
29 platforms.

30 Proximal rift margin areas are characterized by a series of half grabens with footwall and
31 hangingwall dip slopes of shallow lacustrine carbonates and fluvio-deltaic mixed carbonate
32 & siliciclastic deposits in marginal, hangingwall basins. Central areas are carbonate-rich
33 with platforms established over horst blocks surrounded by deeper-water carbonate facies.
34 Distal areas have the highest amount of stretching and subsidence and accumulate the
35 thickest carbonate successions over a template of buried horsts and grabens. The entire
36 carbonate succession underlies a thick layer of Aptian salt, which forms the seal to this
37 prolific hydrocarbon system.

38 Keywords: Pre-salt, lacustrine, carbonate platforms, tectono-stratigraphy, Campos Basin

39 **INTRODUCTION**

40 The lacustrine pre-salt carbonates depositional systems of the Campos and Santos basins
41 are very large, probably unique in the geological record, and have no comprehensive
42 modern analogues. The non-marine, pre-salt stratigraphy of these basins probably
43 accumulated in the largest lacustrine system the world has ever known. The rocks in the
44 Campos Basin host oil and gas reservoirs within mollusk-rich coquinas but also have non-
45 producing microbial or travertine-like carbonate rocks similar to those of the Santos Basin.
46 However, largely because of commercial sensitivities, very little is known on the detail of
47 these rocks. There are very few accessible publications on the thicknesses, stratigraphic
48 geometries, lateral extent, facies, stacking patterns, facies models and environments of
49 deposition. However, there are over 400m (1312ft) of lacustrine carbonate facies
50 encountered in the Coqueiros Formation of the Campos Basin, some of which host large
51 fields (Figure 1) that have been producing oil since the early 1980s (e.g. Badejo and

52 Pampo fields, Guardado et al., 1989). These hydrocarbons are sourced from the
53 underlying thermally mature shales with high organic content within the Coqueiros and
54 Atafona Formations (*cf.* Jiquiá and Buracica units, Guardado et al., 1989). The reservoirs
55 are within lower Aptian coarse-grained molluscan rudstones, or coquinas of the Coqueiros
56 Formation, and are sealed by upper Aptian evaporites of the Retiro Formation (Figure 2).

57 This paper describes and interprets successions along a proximal to distal profile through
58 the syn-rift, pre-salt stratigraphy of the southern Campos Basin. This is based on a
59 Petrobras dataset of 3D seismic and a transect of 12 wells with 400m (1312ft) of core,
60 gamma ray logs and one well with BHI log and sidewall cores.

61 A major result of this study is that carbonate platforms may be formed in large lake
62 systems in continental rift settings. In the Lower Cretaceous of the southern Campos
63 Basin, seismic and well data confirm that the platforms are 100s of meters in thickness
64 and 10s of kms across and that they accumulate over structural highs. These are similar in
65 scale to their marine counterparts and have similar aggrading and prograding geometries.
66 Most of the existing facies and sequence stratigraphic models for carbonate platforms are
67 based on marine carbonate systems, whereas models for non-marine systems are scarce
68 in the current literature. This combined analysis of 3D seismic and well data enables the
69 construction of facies and tectono-stratigraphic models for these lacustrine platforms.
70 These models contribute to the understanding of the Early Cretaceous carbonate
71 successions of the Southern Campos Basin, Brazil, that is needed for further exploration
72 and production but also to assist in the interpretation of the opposing margin offshore
73 southwest Africa where exploration is at an earlier stage (Thompson et al., 2015).

74 The 3D seismic interpretations reveal an oblique, extensional rifting system, characterized
75 by a series of grabens, half-grabens, accommodation zones and horsts oriented NE-SW to

76 NNW-SSW. This structural framework is divided into three proximal to distal tectonic
77 domains based on structural style, stretching factors and subsidence rates. This structural
78 template exerts a strong influence on depositional patterns and sedimentary fill of the late
79 syn-rift Coqueiros Formation and the carbonate platforms differ in these three domains.

80 The sub-surface data analysis indicates 100s of m thick lacustrine carbonate deposits,
81 with fluvio-deltaic mixed carbonate & siliciclastic deposits in marginal areas and pure
82 carbonate platform systems basinward. The dominant carbonate facies in the Barremian
83 and lower Aptian Coqueiros Formation are mollusk-rich rudstones and floatstones that
84 accumulated in open, brackish water, lake system. Ostracods and gastropods occur
85 subordinately. Microbialite-rich facies occur overlying the post-rift unconformity in the
86 middle Aptian Macabu Formation, in more restricted paleoenvironmental conditions. All
87 these carbonate successions are overlain by a thick layer of Aptian evaporite, which
88 concludes the continental sequence of the studied succession.

89 These pre-salt carbonate successions record the break-up of Gondwana and witness the
90 development of rift evolution, which culminate with the opening of the south Atlantic later in
91 the Early Cretaceous.

92

93 **METHODS AND DATA**

94 Seismic horizons and the main faults were mapped using a 3D seismic survey and tied to
95 well data, using Landmark software. The 3D seismic data covers an area of some 7500
96 km² (Figure 1) with 23 wells, mostly concentrated in the shallow water sites in the
97 northwest of the study area in the oil-fields of Pampo, Linguado, Badejo and Trilha. The
98 seismic data were merged ("Big Merge", Figure 1) internally at Petrobras from four pre-

99 stack processed seismic surveys; Alfa, Beta, Gamma and Delta each of them with different
100 acquisition parameters, grid characteristics and frequencies. The grid is arranged in 1300
101 in-lines by 2662 cross-lines with the spacing between them of 50 by 50m (164ft) and an
102 average frequency estimated of 15-18 Hz.

103 Five stratigraphic horizons were mapped throughout the dataset: Top Cabiúnas Fm
104 (basalt, and acoustic basement), base and top Coqueiros Fm (top early and late syn-rift),
105 and base and top Retiro Fm salt (base post-rift) (Figure 3). These picks were based on
106 continuity of the reflectors, seismic facies changes and terminations (onlap, downlap,
107 toplap, etc.). Various seismic attributes were used to assist in the mapping of faults and
108 the best attribute came from dip. 3D views, maps and cross-sections were all used to
109 identify and interpret the tectonic setting, structural patterns, and internal and external
110 geometries of strata in the carbonate-rich units within the late syn-rift Barremian to early
111 post-rift (sag) Aptian succession. Cores and wireline log data through the Coqueiros Fm
112 were studied from 21 wells arranged in a proximal to distal transect (Figure 1) that are tied
113 to the seismic data (Figure 3). The proximal area (Domain I) is sampled in 18 wells from
114 the Pampo, Badejo, Linguado and Trilha oilfields, whilst Domain II is sampled by three
115 wells (19, 20, 21) with BHI logs and sidewall cores together with wireline logs in well 20.
116 The distal area, Domain III, is only known from seismic data. Eight wells were studied in
117 detail with core and electrical logs and a further 13 were used to tie the seismic to
118 electrical logs, 400m (1312ft) of core were logged (1:20 scale), 600m (1968ft) of FMI log
119 were interpreted (1:10 scale) and more than 200 thin sections were studied.

120

121 **GEOLOGICAL SETTING OF CAMPOS BASIN PLATFORMS**

122 **Stratigraphic Setting**

123 The pre-salt carbonates of the Campos Basin are only known from offshore data and form
124 part of the Lagoa Feia Group, which is dated by non-marine ostracod assemblages as
125 early Aptian (Figure 2; Winter et al., 2007). This unit contains reservoirs that have been
126 producing hydrocarbons since the early 1980s and is laterally equivalent to the
127 hydrocarbon-rich Itapena and Barra Velha Fms of the Santos Basin to the south. Both
128 basin-fills contain syn-rift strata laid down during rifting of Gondwana and the early stages
129 of formation of the south Atlantic. The Lagoa Feia Gp is divided into the Itabapoana,
130 Atafona, Coqueiros, Gargau, Macabu and the Retiro formations (Figure 2). The
131 Itabapoana Fm. is characterized of polymict conglomerates, lithic sandstones, siltstones
132 and shales (Rangel et al., 1994) that are associated with the western border faults to the
133 basin in proximal sites. This formation reaches 5km (31,5Mi) thick, rests unconformably on
134 the basalts of Cabiúnas Formation, underlies and is laterally equivalent to the Coqueiros
135 Fm and is interpreted to have accumulated in alluvial fans and deltas near the margins of a
136 syn-rift lacustrine system (Winter et al., 2007).

137 The Atafona Fm comprises mostly sandstones, siltstones and shales interbedded with thin
138 carbonate layers (Rangel et al., 1994). The siltstones and sandstones are rich in talc and
139 stevensite minerals, formed by chemical precipitation associated with hydrothermal activity
140 in alkaline volcanic lakes (Bertani and Carozzi, 1985a, 1985b). The formation lies
141 unconformably on basalts of the Cabiúnas Fm, and underlies and also grades laterally into
142 the Coqueiros Fm. Palynological and ostracod dating indicate these sediments were
143 deposited during the Barremian (Figure 2; Winter et al., 2007), in the early syn-rift phase of
144 basin evolution.

145 The Coqueiros Fm (informally referred to as the Coquina) is represented by interbedded
146 units of lacustrine, mollusk-rich carbonates (coquinas) and shales (Rangel et al., 1994)
147 that occur in the central and distal parts of the study area; lateral to the Itabapoana Fm.

148 The Coqueros Fm comprises hundreds of meter -thick packages of porous molluscan
149 rudstones and floatstones (Thompson et al., 2015). These accumulated in the late syn-rift
150 lacustrine environments of the early Aptian, are the main pre-salt reservoirs of the Campos
151 Basin, and are the major topic of this paper.

152 The top of the Coqueiros Fm is identified in seismic profiles as a prominent post-rift
153 unconformity (Figures 3 and 4) where extensional faults terminate. This surface is
154 onlapped and overlain by the Macabu Formation; represented by microbial carbonates and
155 some siliciclastic units (Rangel et al., 1994; Muniz and Bosence, 2015). These are
156 interpreted to have been deposited in an arid climate alkali lake, in shallowing-upward,
157 lake margin cycles (Muniz and Bosence, 2015). The Gargau Fm. is a marly unit that is
158 laterally equivalent to the Macabu Fm, occurring in more proximal areas.

159 The upper contact of the latter two units is unconformable with the Retiro Formation, the
160 main evaporite unit of the post-rift or sag phase of basin evolution. Based on palynological
161 and ostracod dating, these sediments are reported to be of late Aptian age (Figure 2,
162 Winter et al., 2007).

163 **Tectonic Setting**

164 Tectonic setting is a major control on the morphology, depositional geometries and facies
165 distribution of carbonate platforms in rift basins such as the Barremian and Aptian in the
166 Campos Basin (Platt and Wright, 1991; Guardado et al., 2000; Bosence, 2012). To
167 understand the morphology and internal geometries of such carbonate platforms an
168 integrated study of the tectonics and the stratigraphy is essential. Here we illustrate the
169 tectonic setting for the syn and post-rift (sag phase) carbonates of the southern Campos
170 Basin, using 3D seismic reflection and subsurface well data (23 wells with sonic and
171 gamma ray and neutron logs), as indicated in Figures 4 and 5.

172 The NW to SE dip section through the area (Figure 4) indicates that the basement is cut by
173 extensional faults that continue up through the syn-rift strata with distinctive wedge-shaped
174 infill of half-grabens and grabens. These are filled with the clastic-rich Atafona Fm. The
175 late syn-rift Coqueiros Fm is cut by fewer faults but shows marked thinning over basement
176 highs and thickening into lows.

177 The map of the top basalt (acoustic basement) illustrates the template for the
178 accumulation of the syn- and post-rift sag strata (Figure 5). Most of the structures are
179 arranged in a NE-SW direction. Secondary structures are aligned NNE-SSW.

180 The area has been divided into three basinal domains (Figures 4 and 5). Domain I
181 comprises the Badejo High, a horst of volcanic rocks with a steep, fault-bounded margin to
182 the east. This high contains the Pampe, Linguado, Badejo and Trilha oil fields (Figure 1)
183 and wells 1-18 of this study (Figure 6). Domain II is more complex with a series of
184 polygonal shaped half-grabens bisected by a WSW – ENE accommodation zone with a
185 central horst, or interbasinal ridge (Rosendahl et al., 1986) and an interbasinal high on its
186 eastern margin (External High, Figure 4) where wells 19, 20 and 21 are sited. Domain III to
187 the southeast today forms an extensive low, parallel to the rift margin with a number of
188 linked (NE – SW) half grabens and buried (or relict) horsts.

189 The extensional faults were active for a longer interval distally to the southeast. In proximal
190 areas, Domain DI, they are short lived, and faults appear to terminate in the late syn-rift
191 succession. In Domain DII, the normal faults reach the top of the syn-rift succession.
192 However, in Domain DIII, the normal faults are mostly long-lived and cut the post-rift
193 succession, in some cases reaching to the base salt (Figure 4).

194 The structural elements in the study area define an extensional rifting system. However,
195 the segmented faults, the curved fault segments together with the NNE-SSW border of the

196 basin that is oblique to the orientations of the rift faults (NE-SW), all indicate an oblique
197 extensional rifting system (McKenzie, 1978). Individual half-graben, graben and horsts
198 form the rift system. Basinward, in the SE of the area, the individual half-grabens appear to
199 have linked due to the advanced evolutionary stage of the rift, where they become more
200 symmetric, forming a large graben, with conjugated border faults (Davison, 1999).

201 The early syn-rift accommodation is filled with terrigenous sediments of the Itabapoana Fm
202 in the proximal area and Atafona Fm to the offshore (Figures 2 and 6), possibly in
203 response to high extension rates that appear to have reduced by the time of the late syn-
204 rift stage that are dominated by carbonate sediments. A phase of post-rift uplift and
205 erosion is marked by the post-rift unconformity or “breakup unconformity” (Guardado et al.,
206 2000) of Aptian age. The post-rift, or sag, strata infill any remaining inherited rift-related
207 topography and thicken basinward in response to thermal subsidence of the post-rift
208 phase.

209

210 **SEDIMENTARY FACIES AND FACIES ASSOCIATIONS**

211 **Paleontology and Paleoenvironment**

212 Previous authors have noted the absence of typical stenohaline marine organisms within
213 the Lagoa Feia Gp (Schaller, 1973; Bertani, 1984; Carvalho et al., 1984) and have
214 proposed that the unit was deposited in a fluvio-lacustrine complex. Similarly, Abrahão and
215 Warne (1990) based on open-hole logs, cutting and core samples, proposed three
216 depositional environments for the Lagoa Feia Gp; alluvial fans, exposed lake-margin mud
217 flats, and sub-lacustrine deposits. In this work, a suite of non-marine, semi-infaunal,
218 suspension feeding, bivalves have been recognized; *Angelasina cf. A. plenodonta* Riedel,

219 *Arcopagella, longa* n. sp, *Camposella rosea* n. Gen et n. sp, *Desertella acarenata* n. sp,
 220 *Kobayashites brasiliensis* n. sp, *Remondia (Mediraon) magna* n. sp, *Sphaerium cf. S.*
 221 *ativum* White, *Trigonodus camposensis* n. sp. With the exception of *Sphaerium*, all are
 222 endemic to the Brazilian offshore basins. Pulmonate gastropods (*Limneidae*) are common
 223 and typically found in fresh waters (Carvalho et al., 1995). Non-marine ostracods are
 224 common to locally abundant and are used as biostratigraphic markers within the Lagoa
 225 Feia Gp (Silva-Telles, 1992; Carvalho et al., 1995). Pycnodontid fish of the genus
 226 *Pycnodus* (Gallo, oral communication in Carvalho et al., 1995) are also present and
 227 considered to be a potential predator of the benthic mollusks and some crustaceans
 228 (Carvalho et al., 1995). A vertebrate bone fragment was discovered in Well 2 during this
 229 study. From its internal structure it is interpreted to be either from a crocodylomorphous
 230 reptile or a dinosaur (Dr. A. Kellner, Brazilian National Museum, pers. comm.). However
 231 fresh water algae (e.g. charophytes) have not been observed so it is considered that the
 232 aqueous environments of the Lagoa Feia were brackish water lakes. The Mg- silicate
 233 Stevensite is present in lower levels of the Group indicating an Mg-rich alkali lake
 234 environment (Wright and Barnett, 2015) for the earlier stages of the Campos Basin rift.
 235 Although there are some records of possible marine organisms or biochemical indicators
 236 within this succession (Hessel and Mello, 1987; Silva Telles, 1996) no unequivocal marine
 237 fossils have been seen in the 400m (1312ft) of core or 200 thin sections studied within this
 238 project.

239

240 **Facies descriptions and interpretation**

241 The cores and matching thin sections were used to establish 19 facies based on their
 242 lithologies and fossils. The majority of the cores come from proximal sites of Domain I and

243 the bed-by-bed logging of cores (Muniz, 2013) provides the basis for the facies in this
244 paper. These core-based facies, backed up with thin sections, are described and
245 depositional processes interpreted in Table 1 and the carbonate facies are illustrated in
246 Figure 7. The interpreted depositional settings of the facies is illustrated in a facies model
247 based on a proximal-distal lake margin profile in Figure 8.

248 The more distal sites of the study area have not been cored but are imaged in well 20 with
249 a continuous borehole image log and sampled by some sidewall cores (Figure 9).
250 Together these records enable the identification of borehole image (BHI) facies, and the
251 image log for 400m (1312ft) of the Coqueiros Fm from well 20 are used to extend the data
252 from the cored wells to a more distal area. From the BHI log and sidewall cores from the
253 Macabu Fm in well 20, Muniz and Bosence (2015) described and interpreted 9 BHI based
254 facies (BH1-BH-9); Breccia, Laminated Shale, Marl, Conglomerate, Mudstone, Grain-
255 rudstone, Microbial Laminite, Stromatolite and Thrombolite. Of these, the last three
256 microbial facies do not occur in the Coqueiros Fm. One facies, the Rudstone/coquina
257 (FMI-7 in Muniz, 2013) is in addition to those in the above list, and occurs in abundance in
258 the Coqueiros Fm in well 20. This BHI facies is relatively conductive with a coarse, grainy
259 appearance, visible bivalve shells and pores represented by dark brown patches (Figure
260 9). This lithology occurs in plane or cross-bedded units that are up to 10s of meters in
261 thickness and is very similar to the Rudstone facies (Rc, Rt, and Rm) of the cored material,
262 and is similarly interpreted to have formed in high energy, shallow lacustrine environments
263 (Table 1).

264 The facies are grouped into 4 facies associations (FA) based on their environment of
265 deposition. Two of these associations (Alluvial Fan & Plain FA and Delta & Delta Margin
266 FA) are dominated by siliciclastic sediments from the proximal Itabapoana Fm. Two, from

267 the Coqueiros Fm, are carbonate or mixed carbonate-siliciclastic sediments of the Deep
268 Lacustrine FA and the Lacustrine Carbonate Platform FA and are the focus of this paper.
269 The occurrence of the facies of the latter two associations on a proximal to distal lake
270 profile is illustrated in (Figure 10) and the occurrence of the facies associations is
271 discussed below.

272 **Alluvial Fan and Plain Facies Association (AF&P-FA)**

273 This association comprises the clast-supported conglomerate (CB) and coarse sand (Sc)
274 facies that are represented in wells 1 and 2 in the proximal part of the basin (Figures 6 and
275 10). These sedimentary deposits are interpreted to be associated with braided fluvial
276 systems and alluvial fans that act as a conduit for the transport of polymictic terrigenous
277 sediments into the basin. The alluvial fans and plains occur westwards and proximal to the
278 main lacustrine environments in the hanging wall sub-basin, close to the border fault.

279 **Deltaic and Delta Margin Facies Association (D&DM-FA)**

280 This association is interpreted to occur on the western border of the lacustrine system
281 (Wells 1 and 2), where distal alluvial systems enter the aqueous environment. It comprises
282 siliciclastic deltas at the mouths of rivers together with the delta slope, and mixed
283 carbonate-siliciclastic shoreface deposits marginal to the delta. The siliciclastic facies are
284 represented by medium to fine grained sands (Sf, Sm) interpreted to have formed in the
285 distributary channels of the deltaic system. The finer grained facies of this association are
286 considered to be channel-levee and delta plain deposits, and are predominantly
287 represented by siltstone and shale (ST, SH) facies. Similarly, this association also
288 comprises the more distal portions of prodelta and delta front, with deformed and slumped
289 deposits of matrix supported conglomerates (CM), and also thin and very thin units of sand
290 (Sm, Sc) and rudstone facies that are interpreted to have formed in a deep lake

291 environment as turbidites. This is based on characteristic sharp erosional bases with load
292 and flame structures in the base of the beds. In the lateral marginal portion of the deltas,
293 sandy shoreface deposits may be reworked and pass laterally into mixed carbonate-
294 siliciclastic deposits such as bioclastic-rich sandstones (Sf, Sm, Sc) or grainstones (G),
295 packstones (P) and rudstones (Rt) with terrigenous grains. These shelly shoreface
296 deposits also occur on the delta top (e.g. Well 1, Figure 10) and may be reworked as
297 turbidites on the delta slope.

298 **Deep Lacustrine Facies Association (DL-FA)**

299 This association comprises interbedded siltstones, mudstones and shales, and in distal
300 sites by fine grained carbonate facies such as mudstone (MD), Marl (ML) and wackestone
301 (WK). These facies are interpreted as having formed in the deepest subaqueous
302 sedimentary environment of the continental rift system (Figure 10). Most of it occurs below
303 storm wave base, in the hypolimnium zone, where there is evidence of low-oxygen
304 conditions such as preservation of organic matter and laminated muddy mudstones (MD)
305 and marls (ML). Commonly these deposits are characterised by the abundance of
306 ostracods. Close to the toe of the slope of the delta front, turbidite deposits may also occur
307 (Wells 1 and 2, Figures 6 and 10).

308 **Lacustrine Carbonate Platform Facies Association (LCP-FA)**

309 Shallow lake environments isolated from siliciclastic supply commonly accumulate thick
310 successions (hundreds of meters) of bioclastic carbonates (Figure 10). These are referred
311 to as high energy ramp margin type by Platt and Wright (1991), but because of the
312 thickness (100s m) and lateral extent (10s km), the range of facies and different structural
313 settings developed in the Campos Basin (Domains I – III), these accumulations are
314 regarded as carbonate platforms in their own right (*cf.* Buckley et al., 2015). Rudstones,

315 grainstones and floatstones of bivalves (Rm, Rt, Rc, G, F) dominate and, less commonly,
 316 gastropod or oncolid rudstones occur. The rudstones are plane or cross-bedded and
 317 commonly stacked in packages up to many tens of meters in thickness and are interpreted
 318 to form shallow high-energy bank and bar facies within these platforms. Also included in
 319 this facies association are the thick successions of Rudstone/coquina interpreted from the
 320 BHI logs and sidewall cores in well 20. Facies with *in situ* bivalves preserved in a muddy
 321 matrix (Rm, Figure 7J) are considered to have accumulated in deeper, quieter water
 322 settings. These shallow-water facies pass laterally into the deeper lake deposits with lower
 323 energy facies such as thinner beds of bioclastic packstones (P), wackestones (WK) and
 324 mudstones (MD) or floatstones (F), which are commonly ostracod-rich (Figures 8 and 9).

325

326 **METER-SCALE SEDIMENTARY CYCLES**

327 In cored successions of the Lacustrine Carbonate Platform FA from wells 7, 8 and 12
 328 (Figure 6) in the central part of the study area, carbonate facies are arranged in meter-
 329 scale cycles. Logged intervals show repeated arrangements of facies, typically in
 330 shallowing-upward successions, consistent with the proposed facies model (Figures 8 and
 331 11). Cycles comprise subaqueous carbonate facies bounded by brecciated, Fe stained
 332 surfaces (Facies Bk, Figure 7A) that are interpreted as forming in emergent conditions
 333 (Table 1, Figure 8). These surfaces are overlain by thin beds (with or without ostracods) of
 334 interbedded green/grey siltstone (ST), shale (SH), wackestone (Wk), packstone (P),
 335 grainstone (G) and molluscan rudstones comprising about 1 meter (3,2ft) in total
 336 thickness. The major part of the cycles comprises 2-10m (6,6-32,8ft) of grainstone (G) and
 337 rudstone facies (Rm, Rc) (Figure 11) that are capped by emergent surfaces.

338 The fine-grained clastic intervals, that commonly show a positive spike on the gamma log,
339 are interpreted as lowstand and transgressive deposits whilst the higher energy rudstone
340 intervals, some with cleaning-up gamma trends, represent highstand deposits reflecting
341 higher energy, shallow-water molluscan production. The cycles are interpreted as
342 accumulating from progradation of high-energy lake margins, or bars during repeated
343 periods of lake flooding.

344 The variation in cycle thicknesses and lithologies preserved, together with observations of
345 desiccation cracks and brecciation developed in low energy, subaqueous facies indicate
346 irregular and rapid changes of lake level. In this setting lake level might be controlled by
347 structural or hydrological/climatic changes and no attempt is made to resolve these
348 controls or to correlate these meter-scale cycles between wells.

349

350 **TECTONO – SEDIMENTARY MODELS**

351 As discussed above, the study area in the southern Campos Basin, has been divided into
352 three different tectonic domains: DI, DII and DIII (Figure 12). In this section the structural
353 settings are integrated with the sedimentological data to generate tectono-sedimentary
354 models for each of the three Domains.

355

356 **Tectono-stratigraphic model- Tectonic Domain I**

357 **Domain I includes** the Pampo, Badejo, Linguado and Trilha oil fields and a proximal half-
358 graben landward of the Badejo High (Figure 5). Here, a series of half-grabens occur with a
359 syn-rift stratigraphy that thickens westwards to the basin border fault and thins to the east
360 onto the Badejo High. Accommodation is provided by both synthetic and antithetic

361 extensional faults. The lateral displacement of the normal faults suggests a crustal
362 stretching β value, of 1.24 ($\beta = a'/a$ – where a' =deformed length a = original length). Within
363 the late syn-rift Coqueiros Fm in proximal areas both siliciclastic and carbonate sediments
364 occur indicating it is close to the siliciclastic source area. Siliciclastic sediments may
365 predominate in the hangingwall depocentres (e.g. well 2) whereas carbonates occupy the
366 two main horsts (wells 5 and 6) as examples of fault-block carbonate platforms (Figure
367 13). However, it should be recognized that the Lacustrine Carbonate Platform - Facies
368 Association (LCP-FA) extends into the more distal half-graben sub-basins (wells 1, 7, 8,
369 Figure 6) indicating that rift related topography was filled at these times and also that
370 clastic supply did not reach the more distal areas. Conversely, stratigraphically thinned
371 horst sites may accumulate Deep Lacustrine - Facies Association (DL-FA) indicating
372 flooding of these basement highs by lacustrine waters. During the Barremian the proximal
373 half-graben was partially filled with sediment from the Delta and Delta Margin- FA (wells 1
374 and 2, Figures 6 and 10) that are locally redeposited as sub-lacustrine fans. Later, during
375 the Aptian, Alluvial Fan and Plain - FA of conglomerates and sandstones occur in both
376 half-graben and footwall sites. The facies successions suggest proximal alluvial fan
377 systems evolve basinward to braided fluvial systems and Gilbert-type deltas in lacustrine
378 environments (Figure 13). Within this proximal dominantly clastic system this bench-type
379 carbonates accumulated (*cf.* Wright, 1992). These comprise bioclastic carbonate
380 sediments accumulating in mixed carbonate-siliciclastic beaches, beach ridges, and also
381 mollusk-rich subaqueous bioclastic bars and shore face deposits (Figure 13). The more
382 distal horsts of the Badejo High are relatively clastic-free and extensive and thick
383 amalgamated packages of bioclastic carbonates of the LCP –FA accumulated mainly in
384 shallow, high-energy sites. Ramp-like profiles to these platforms are interpreted to have

385 accumulated on hangingwall dip slopes whilst steeper slopes, with reworked facies are
386 interpreted for footwall sites.

387 The distribution of the facies associations between hanging wall and footwall sites for this
388 half-graben attached to the rift border fault has many similarities to a terrestrial to shallow
389 marine analogue in the Miocene of the Gulf of Suez (Cross and Bosence, 2008)

390

391 **Tectono-sedimentary model- Tectonic Domain II**

392 The second platform type occurs in the intermediate area of the Campos Basin in the
393 region of Espadarte oil field (Figure 1), where synthetic and antithetic half-grabens are
394 divided by an accommodation or transfer zone (Figures 4 and 13), with an associated
395 horst, or interbasinal ridge (Rosendahl et al., 1986). Stretching values (β) are estimated at
396 1.40 (Figure 12). This domain has a complex geometric arrangement of acoustic
397 basement (Figures 4 and 5). The geometries of the carbonate platforms are aggradational
398 on interbasinal highs and clinofolds are seen prograding outward from these highs into
399 half-graben depocentres, with a polygonal or rhombic style in plan view (Figure 14). On the
400 interbasinal ridge, thick packages of high energy, bioclastic carbonate banks and bars are
401 interpreted based on a similar gamma response to the cored and imaged Lacustrine
402 Carbonate Platform FA in adjacent wells 19 and 20 (Figure 14). These strata are
403 seismically chaotic (Figure 12a, well 19) but appear to have accumulated in an
404 aggradational style. Laterally to this high shallow lacustrine sediments are seen to
405 prograde southeast and northwest into surrounding lows. The progradational geometries
406 are evident at two levels; they are imaged as large seismic scale geometries but also
407 interpreted from coarsening-upward profiles in wireline logs from well 19 and also in core
408 from well 12 (from Deep Lacustrine to Lacustrine Carbonate Platform FA) and BHI logs

409 (Muniz 2013). In the interior of the banks, beside the horst block, the seismic sections
410 show aggradational parallel and divergent seismic geometries. This seismic facies is
411 interpreted to reflect low energy mud-rich carbonate sediments such as marls, mudstones
412 or even shales (between wells 12 and 19, Figure 14).

413 Domain II is limited to the west by the prominent Badejo High and to the east by the
414 External High, which is a regional hinge zone (Figures 4, 5 and 13). The depositional
415 system appears to be isolated from clastic supply and accumulates autochthonous and
416 parautochthonous bioclastic carbonates. These are transported and locally reworked
417 mainly by storm and wave processes as evidenced by the commonly occurring, high
418 energy, Lacustrine Carbonate Platform FA. Hundreds of meters of Aptian bioclastic
419 carbonates accumulated in sub-basins with large amounts of accommodation space
420 (Figure 14). In this context, bioclastic sediments commonly accumulated in progradational
421 sets in the area of well 20 indicating that even stratigraphically thickened sections all
422 accumulated in relatively shallow water, but with episodes of flooding resulting in
423 accumulation of sections of Deep Lacustrine FA with their higher Gamma values.
424 Therefore the productivity of these molluscan carbonate communities appears to have
425 exceeded the accommodation space maintaining keep-up and progradational, shallow
426 facies, locally exhibiting subaerial exposure surfaces in cores.

427 **Tectono-sedimentary model- Tectonic Domain III**

428 The third region, in the most distal part of the study area, has the highest degree of
429 stretching (estimated β factor of 1.59) and asymmetric half-grabens are linked to form a
430 large symmetrical graben with some relict horsts. These form highs and the template for
431 what are interpreted from seismic data only as unattached carbonate platforms (Figures 5,
432 12 and 15).

433 There is considerable thickening of the Early Cretaceous strata in this distal area in
434 response to a higher rate of stretching and subsidence. Relict horsts formed morphological
435 highs that acted as the basement for what are interpreted as unattached, or isolated,
436 carbonate platforms that are kms across and 100s of meters in thickness (Figures 12 and
437 15). There are no wells in this area and the interpretation is based solely on the
438 progradational seismic geometries radiating from the highs. These are unlikely to be
439 clastic progradational features as there is no source area for clastic supply and
440 progradation is interpreted radially out from the structure. Seismic lines show progradation
441 of interpreted platform carbonates (LCP-FA?) with lenticular / sigmoidal geometries into
442 deeper basinal areas and these are overlapped by interpreted deep basinal sediments (DL-
443 FA?) with aggradational parallel reflectors (Figure 12). On the platform top aggradational
444 and also chaotic seismic facies are seen (Figure 12). If these horizons are traced to the
445 nearest and more proximal wells (wells 12 and 20) then the lower portion of aggradational
446 and progradational seismic geometries are interpreted to be molluscan rudstones and
447 grainstones (LCP-FA) and upper portion as microbialite facies as described from well 20
448 by Muniz and Bosence (2015).

449

450

451 **DISCUSSION**

452 **Hydrological controls**

453 Whilst the morphology of this lake or lake system is still unknown there are some
454 indicators of its extent and likely connectivity. Despite the unavailability of a detailed
455 biostratigraphy for the wells in this study, there are lithological similarities between the sub-
456 basins studied along this NW – SE transect (Figure 6). Cored lithologies and gamma and

457 BHI log responses indicate that correlations at the facies association level can be made
458 between the sub-basins indicating a common sedimentological history and likely
459 connection during the late syn-rift and post-rift (sag) phases. There is no evidence in the
460 form of evaporitic intervals to suggest isolation or closure of parts of the lake system. The
461 conclusion is that this transect represents a section through a connected through-flowing
462 lacustrine system of at least 150 km (93.2Mi) across.

463 The core logging, thin section and facies analysis indicates paragenesis of a progressive
464 change through time in the Lagoa Feia lake hydrology, from alkaline in the lower
465 sequences, to fresh water, to brackish waters and finally hypersaline in the upper
466 successions with the Aptian salts (Figure 9). The lower coquina succession comprises
467 rudstones rich in bivalves but also with ostracods and grains of stevensite, a tri-octahedral
468 Mg silicate. Stevensite is characteristic of alkaline lake waters, commonly derived from
469 volcanic source areas (Cerling, 1994; Wright, 2012). A flooding event depositing
470 widespread shales, the main source unit for the Campos Basin, separates these lower
471 coquinas from the thick overlying bivalve rudstones and grainstones of the lacustrine
472 Carbonate Platform Facies association. These deposits have a higher diversity of bivalves
473 but charophytes appear to be absent. The bivalves are various taxa of the family
474 Unionidea, many are new species, some new genera, which appear to be endemic to the
475 south Atlantic so their specific environmental tolerances are, as yet, not fully understood.
476 However, we have found no equivocal marine taxa in the cores or thin sections we have
477 studied. Similarly, we have found no horizons with evaporite minerals indicating isolation
478 and hypersalinity. Taken together, these palaeoenvironmental indicators imply brackish
479 water conditions for the accumulation of this unit.

480 Towards the top of the Lagoa Feia Gp., Hessel (1993) records a decrease in diversity of
481 bivalves, but an increase in the abundance of gastropods and this is also found in this

482 study (Figure 9). A shift to more closed lake conditions in this late syn-rift succession in a
483 well 2km (1.24Mi) to the west of well 5 is proposed by Silva Telles (1996) based on the
484 Talbot (1990) model of a positive correlation of $\delta^{13}\text{C}$ and $\delta^{18}\text{O}$ isotopes (see discussion in
485 Muniz and Bosence, 2015). A radical environmental change is indicated at the post-rift
486 unconformity as the molluskan communities of the Coqueiros Fm disappear to be replaced
487 by microbial carbonates of the Macabu Fm. These are associated with coarse carbonate
488 grainstones, comprising ooids, spherulites, stevensite grains, quartz and feldspar
489 suggesting a return to alkali Mg-rich lake waters (Muniz and Bosence, 2015). A 2 per mil
490 positive shift to heavier oxygen isotopes over the post-rift unconformity followed by a
491 continuing positive trend up to the base of the evaporites indicates increasing salinity and
492 desiccation of the lake system. This succession underlies a thick layer of Aptian age salt
493 that records evaporation of the lake system and closure of the continental record in the
494 Campos Basin.

495 **The Coquina Facies (LCP Facies Association)**

496 A facies model for the carbonate facies of the Coqueiros Fm. is presented which integrates
497 shallow and deep lacustrine facies associations. This has similarities to the wave-
498 influenced ramp-type margin of Wright (1990). However, in the Campos Basin, the high
499 energy shallow facies are dominated by molluskan (in particular bivalve) grainstones and
500 rudstones. These pass through deeper waters below storm wave-base into wackstones,
501 marls and shales with abundant ostracods (Figure 9). The dominance of endemic, non-
502 marine bivalve taxa within this eponymous formation has been documented by many
503 authors (e.g. Guardado et al., 1989; Abrahão and Warme, 1990; Carvalho et al., 2000 and
504 Thompson et al., 2015). All authors are agreed that the bivalve accumulations represent
505 high energy, shallow lacustrine sites and that there is variability in size, sorting and matrix
506 within the coquinas. In this study we found the Dunham (1962) classification modified by

507 Embry and Klovan (1971) enables the broad range of facies in these unusual rocks to be
508 classified. Quieter water, deeper or shallow protected sites accumulate molluscan
509 wackestones and floatstones whilst higher energy sites, grainstones and rudstones. The
510 rudstones are diverse and range from clean-washed rudstones with variable amounts of
511 cement and pore types to rudstones with a coarse terrigenous matrix. Others rudstones
512 have a muddy matrix and a higher proportion of articulated bivalves, some preserved in
513 original life position suggesting a more autochthonous facies (Muniz, 2013). The reworked
514 grainstones and clean rudstones preserve the best porosity comprising interparticle,
515 mouldic, vuggy and some fracture porosity. When stacked in meter to tens of meter-thick
516 successions, these form the best quality reservoir facies.

517 This combined study of seismic data and core indicate that the grainstone and rudstone
518 facies in the Lacustrine Carbonate Platform facies association reach hundreds of meters in
519 thickness and that these accumulate on basement highs but also build out into structural
520 lows within the late syn-rift phase. These molluscan communities formed shallow
521 carbonate platforms on a scale that is unknown elsewhere in the geological record. It is
522 therefore instructive to consider what conditions gave rise to these unique stratigraphic
523 thicknesses of molluscan lacustrine limestones. The late syn-rift stratigraphy is about
524 200m (656ft) in thickness in the proximal area (Domain I) with marginal interbedded
525 clastics and localized thinning over basement highs which accumulate LCP and DL facies
526 associations. However, the late syn-rift succession reaches about 400m (1312ft) in more
527 offshore areas (Domain II), of which about 300m (984ft) is interpreted from a BHI log in
528 well 20 to be shallow-water LCP facies association and 100m (328ft) of DL facies
529 association. The Coqueiros Fm is considered to have accumulated over 8.0 myr from 125
530 to 117 Ma (Winter et al., 2007 – Figure 2) which gives accumulation rates in the southern
531 Campos Basin in the range of 32-50m / myr (32-50m / myr 105-164ft / myr). When

532 compared to accumulation rates of shallow- marine tropical carbonates both Sadler (1999)
533 and Schlager (2005) give an upper limit of approximately 100m / myr (328ft / myr) and an
534 average of about 10m / myr (32,8 ft /myr) , when measured at a similar million-year scale.
535 Accumulation rates are a function of carbonate production, subsidence, transport and
536 compaction as well as the time-scale of measurement. Subsidence rates for the southern
537 Campos Basin may be taken from the thickness of these high-energy, shallow water
538 carbonates (ie 32-50m / myr 105-164ft / myr) which are within the range for other passive
539 margin basins (cf. Einsele, 1992), transport rates are not considered significant as the
540 stratigraphy comprises both shallow and deep water facies and thin-section observations
541 suggest compaction is minimal, however stylolites and solution seams are locally present
542 in some of the cores (Figure 7D). These figures therefore suggest that the production rates
543 from these lacustrine bivalve communities were exceptionally high and similar to marine,
544 shallow-water, tropical carbonate production. Such high rates can only be confirmed with
545 detailed analysis of abundance and growth rates of the preserved *in situ* bivalve
546 communities that would require exceptional preservation conditions.

547 **Tectono-stratigraphic models**

548 Three tectono-stratigraphic models are presented for the three tectonic domains
549 interpreted for the southern Campos Basin. These build on the earlier depositional models
550 of Guardado et al. (1989) and Carvalho et al. (2000) that showed rift margin interfingering
551 of carbonate and clastic facies and more distal bioclastic bars and banks related to horst
552 blocks.

553 The lacustrine carbonate platforms in the proximal Domain I in the Campos Basin are kms
554 in length and width and up to 150m (492ft) thick (Figures 6 and 14). These are interpreted
555 to show many similarities with their counterparts in marine rift basins such as the Miocene
556 of the Gulf of Suez (Cross and Bosence, 2008). Here, shallow-water carbonates

557 accumulate on horsts and footwall highs and, where clastics dominate along the rift border
558 fault and adjacent hangingwall basin in this “margin-attached” (*sensu* Cross and Bosence,
559 2008) setting. Comparison with carbonate sediments generated by a photozoan marine
560 factory seem justified in that the molluskan facies forming the bulk of the coquinas have
561 evidence of being the shallowest, and the highest producing, carbonate facies.
562 Comparison with examples from modern lacustrine environments seem less instructive
563 because whilst some similar mollusk-rich facies may be documented as in Lake
564 Tanganyika (Cohen and Thouin, 1987) and Lake Turkana (Soreghan and Cohen, 1996)
565 from the East African rift, they appear to be thin accumulations and the occurrence and
566 stratigraphic geometries of the carbonate facies association are not known. The East
567 African lake waters are not carbonate-rich and this may be a major limitation to the
568 accumulation of thick packages of carbonate sediments (Cohen, 1989).

569 In Domain II platforms develop around basement highs associated with transfer zones. We
570 have found no similar configurations of tectonic setting and thick lacustrine carbonate
571 deposits in the literature and this appears to be a new type of lacustrine carbonate
572 platform for the continental rift environment. Marine Miocene carbonate platforms in the
573 Gulf of Suez rift, however, show the aggradational and progradational accumulation of
574 carbonates in the transfer zone in the Wadi Kharaza area of Abu Shaar (Cross and
575 Bosence, 2008). In the southern tip to Abu Shaar the accommodation zone accumulates
576 up to 200m (656ft) of shallow marine and slope facies carbonates that prograde to the
577 south into the accommodation zone.

578 In Domain III an isolated platform is interpreted surrounded by deeper lacustrine facies.
579 Isolated microbialite buildups are found in modern lake systems such as Pyramid Lake,
580 USA and in the tufa pinnacles in Mona Lake, USA (Della Porta, 2015) but these are of a
581 much smaller in scale than the platforms described here. Similar scaled lacustrine

582 platforms are described from the pre-salt of the adjacent Santos Basin to the south on the
583 Terminal Horst and the Peroba and Lula (or Tupi) highs (Buckley et al., 2015). These are
584 also sited on basement horsts that are unattached from the rift basin margin. It should also
585 be noted that similar platform morphologies are seen in marine isolated platforms sited on
586 fault blocks not attached to the basin margin in extensional basins such as the Red Sea
587 (Purser et al. 1998) and southeast Asia (Wilson, 2002). The geometries of the two platform
588 systems are rather similar despite the major differences in facies and environments. This
589 is taken to reflect the similar tectonic setting of offshore fault-bounded highs but also the
590 similarities in the Lagoa Feia molluscan carbonate factory with marine photozoan
591 carbonate production. Both carbonate factories have high rates of production in shallow-
592 waters producing either coarse carbonate grains or in-situ buildups, both of which result in
593 semi-autochthonous or autochthonous accumulations that are not transported far from
594 their site of production.

595 A recent paper by Goldberg et al. (2017) proposes a different sedimentary model for the
596 Lagoa Feia Gp of the Campos basin based on more localised 2-D seismics and cored
597 wells from the proximal part of the basin (our Domian I). Their findings support a model of
598 predominantly re-sedimented carbonate and mixed carbonate-siliciclastic sediments as
599 deeper-water deposits that they extend to the broader Campos Basin. Whilst this work is in
600 agreement with our interpretations of facies for these proximal areas our seismic and core
601 data comes from a larger area including rift margin attached and detached half graben
602 basins and includes large areas and thicknesses of shallow lacustrine carbonate facies.
603 These being the source areas for the shallow lake margin carbonate factory. Our
604 sedimentological models are supported by the abundance of tractive structures within the
605 rudstones and grainstones (Table 1), evidence of extensive reworking (abrading and
606 rounding of bioclasts, Figure 7), and the commonly observed and logged arrangement of

607 facies in meter-scale, shallowing-upward cycles capped by emergent surfaces (Figure 11,
608 Muniz, 2013).

609 The integration of data in this study from seismic scale through to wireline log to core-
610 based observations and logging provides relatively robust models for the Campos Basin
611 that can be used in future exploration of the lacustrine successions.

612

613 **CONCLUSIONS**

614 1) The Coqueiros Formation of the Lagoa Feia Group of the southern Campos Basin,
615 Brazil comprises up to 400m (1312ft) of mollusk-rich limestones, coquinas, extending for at
616 least 100km (62Mi) through a proximal to distal transect.

617 2) This dominantly carbonate formation accumulated in the late syn-rift phase of Early
618 Cretaceous rifting of the southwest Atlantic margin in an oblique extensional rift system
619 with faults trending northeast – southwest with a NNE-SSW rift border.

620 3) There are three main structural domains within the rifted margin; a proximal Badejo
621 High is a horst block bounded by half graben and hosts producing oil fields, a central
622 domain, characterized by a mosaic of polygonal half-grabens bisected by a WSW-ENE
623 accommodation zone with a central horst and an offshore domain of linked half-graben
624 and buried horsts, which is in deep water today.

625 4) A similar stratigraphy can be traced throughout the syn- to post-rift (sag) from
626 proximal to distal areas despite this structural complexity suggesting that they formed
627 linked lacustrine basins.

628 5) The bivalve, gastropod and ostracod communities, together with an absence of
629 charophytes, and also evaporites, all suggest an overall brackish water lacustrine
630 environment for the accumulation of these rocks.

631 6) Over 400m (1312ft) of cored wells together with one BHI log and sidewall cores
632 from the proximal to distal transect penetrate a large number of lithologies and 9
633 carbonate, 7 siliciclastic and 3 diagenetically and tectonically modified facies are described
634 from four facies associations; Alluvial Fan and Plain, Deltaic and Delta Margin, Deep
635 Lacustrine and the Lacustrine Platform Facies Associations.

636 7) Proximal areas show interbedding of siliciclastic and carbonate facies whilst distal
637 sites are purer carbonate. Lacustrine Platform FA characterize structural highs and Deep
638 Lacustrine FA the lows. However the platform facies may prograde into and infill some
639 structural lows.

640 8) The facies within the Lacustrine Platform Facies Association are commonly
641 arranged in meter-scale cycles that show both deepening and shallowing phases and are
642 capped by emergent surfaces. In this syn-rift setting lake level can be controlled by a
643 complex of factors such as structural history, climate and fluvial dynamics but these cannot
644 be resolved with our widely spaced wells and with no detailed biostratigraphy.

645 9) Different types of carbonate platforms are found in the different structural domains
646 with a strong tectonic control on facies and geometries; proximal areas are attached to the
647 rift margin and have platforms developed as rectilinear structures on footwall highs to fault
648 blocks with steeper footwall slopes and gentle hangingwall dip slope ramps into clastic-
649 filled half graben, the central zone has a transfer zone with an interbasinal ridge/horst
650 which forms the core for an associated rectilinear platform that progrades into surrounding
651 structural lows, and the offshore domain, with the highest stretching factors and
652 subsidence rates has a buried horst that acts as a template for a large unattached
653 carbonate platform or bank.

654 10) The lake chemistry is considered to change through time from a lower interval of
655 Mg rich alkali lake (with stevensite) to the main part of the late syn-rift with through-flowing

656 brackish lake waters dominated by non-marine molluscan and ostracod taxa but with no
657 charophytes and no evaporite minerals. The post-rift sag succession, following a regional
658 unconformity, is dominated by microbial carbonates of the Macabu Formation with
659 associated spherulites and stevensite and is interpreted to return to Mg- rich alkali waters
660 prior to evaporation and accumulation of late Aptian salts.

661 11) The Coqueiros Fm has carbonate platforms of various types, but with a strong
662 tectonic control on their siting, morphology and facies associations. They are similar in
663 scale to their marine counterparts and surprisingly the accumulation rates are similar to
664 those recorded for marine tropical carbonate platforms.

665

666 REFERENCES

667 Abrahão, D., and J. E. Warme, 1990, Lacustrine and associated deposits in a rifted
668 continental margin – Lower Cretaceous Lagoa Feia Fm., Campos Basin, Offshore Brazil.
669 *in* B. J. Katz, ed., Lacustrine basin exploration, case studies and modern analogs. Tulsa,
670 AAPG, Memoir 50, p. 287-305.

671 Bertani, R. T., 1984, Microfacies, depositional models and diagenesis of Lagoa Feia
672 Formation (Lower Cretaceous), Campos Basin, Offshore Brazil: Ph.D. thesis, University of
673 Illinois at Urbana-Champaign, 199 p.

674 Bertani, R. T., and A. V. Carozzi, 1985a, Lagoa Feia Formation (Lower
675 Cretaceous), Campos Basin, Offshore Brazil - Rift valley stage lacustrine carbonate
676 reservoirs: *Journal of Petroleum Geology*, v. 8, p. 37-58.

677 Bertani, R. T., and A. V. Carozzi, 1985b, Lagoa Feia Formation (Lower
678 Cretaceous), Campos Basin, Offshore Brazil - Rift valley stage lacustrine carbonate
679 reservoirs: *Journal of Petroleum Geology*, v. 8, p. 199-220.

680 Bosence, D. W. J, 2012, Carbonate-dominated marine rifts, *in* D. G. Roberts and A.
 681 W. Bally, eds., *Phanerozoic Rift systems and Sedimentary Basins*: Amsterdam, Elsevier,
 682 p. 89-114.

683 Buckley, J., D. W. J. Bosence, and C. Elders, 2015, Tectonic setting and
 684 stratigraphic architecture of an Early Cretaceous lacustrine carbonate platform, Sugar Loaf
 685 High, Santos Basin, Brazil. *in* D. W. J., Bosence, K. Gibbons, D. P. Le Heron, W. A.
 686 Morgan, T. Pritchard, and B. Vining, eds., *Microbial Carbonates in Space and Time:*
 687 *Implications for Global Exploration and Production*: Geological Society, London, Special
 688 Publications, nº. 418. p. 175 – 191.

689 Carvalho, M. D., M. Monteiro, A. M. Pimentel, H. A. A. A. Rehim, and A. J. Dutra,
 690 1984, Microfácies, diagenese e petrofísica das coquinas da Formação Lagoa Feia em
 691 Badejo, Linguado e Pampo – Bacia de Campos – Projeto 03.01.02, Evolução diagenética
 692 dos reservatórios carbonáticos da formação Lagoa Feia, Bacia de Campos, Rio de
 693 Janeiro, Petrobras. Unpublished Petrobras internal report, 130p.

694 Carvalho, M. D.; U. M. Praça, J. L. Dias, A. C. Silva-Telles Jr., P.Horschutz, M. H.
 695 Hessel, M. Hanashiro, M. S. Scuta, A. S. C. Barbosa, L. C. S. Freitas, A. D. Sayd, 1995,
 696 Coquinas da formação Lagoa Feia da bacia de Campos estudo sedimentológico na
 697 caracterização da qualidade de reservatório: Petrobras Internal Report, Rio de Janeiro,
 698 188 p.

699 Carvalho, M. D., U. M. Praça, A. C. Silva-Telles Jr., R. J. Jahnert, and J. L. Dias,
 700 2000, Bioclastic carbonate lacustrine facies models in the Campos Basin (Lower
 701 Cretaceous), Brazil. *in* E. H., Gierlowski-Kordesch and K. R. Kelts, eds., *Lake Basins*
 702 *through space and time*: AAPG, *Studies in Geology* 46, p. 245-246.

703 Cerling, T. E., 1994, Chemistry of closed basin lake waters: a comparison between
 704 African Rift Valley and some central North American rivers and lakes. *in* E. H., Gierlowski-

- 705 Kordesch and K. R. Kelts, eds., The global geological record of lake basins: AAPG.
706 Studies in Geology, n° 46, p. 245-246.
- 707 Cohen, A. S., and C. Thouin, 1987, Nearshore carbonate deposits in Lake
708 Tanganyika: *Geology*, v. 15, p. 414–418.
- 709 Cohen, A. S., 1989, Facies relationships and sedimentation in large rift lakes and
710 implications for hydrocarbon exploration: examples from lakes Turkana and Tanganyika:
711 *Palaeogeography, Palaeoclimatology, Palaeoecology*, v. 70, p. 65–80.
- 712 Cross, N. E., and D. W. J., Bosence, 2008, Tectono-Sedimentary models for rift-
713 basin carbonate systems: *in* J., Lukasik and J. A. Simo, eds., Controls on Carbonate
714 Platform and Reef Development. SEPM, Special Publication n°. 89, p. 83-105.
- 715 Davison, I., 1999, Tectonics and hydrocarbon distribution along the Brazilian South
716 Atlantic margin, *in* N. R. Cameron, R. H. Bate, and V. S. Clure, eds., The oil and gas
717 habitats of the South Atlantic: The Geological Society, London, Special publication 153, p.
718 133-151.
- 719 Della Porta, G., 2015, Carbonate build-ups in lacustrine, hydrothermal and fluvial
720 settings: comparing depositional geometry, fabric types and geochemical signature. *in* D.
721 W. J. Bosence, K. A. Gibbons, D. P. Le Heron, W. A. Morgan, T. Pritchard, and B. A.
722 Vining, eds., *Microbial Carbonates in Space and Time: Implications for Global Exploration*
723 *and Production*. Geological Society, London, Special Publications 418, p. 17-68.
- 724 Dunham, R. J., 1962, Classification of carbonate rocks according to depositional
725 texture. *in* W. E. Ham, ed., *Classification of Carbonate Rocks*: AAPG, Memoir 1, p. 101-
726 121.
- 727 Einsele, G., 1992, *Sedimentary Basins. Evolution, Facies, and Sediment Budget*.
728 Berlin, Springer-Verlag, 628 p.

729 Embry, A. F., and J. E. Klovan, 1971, A Late Devonian reef tract on northeastern
730 Banks Island, North West Territories: *Bulletin of Canadian Petroleum Geology*, v. 19, p.
731 730-781.

732 Goldberg, K., J. Kuchle, C. Scherer, R. Alvarenga, P. L. Ene, G. Arlementi, L. F. De
733 Ros, 2017, Re-sedimented deposits in the rift section of the Campos Basin. *Marine and*
734 *Petroleum Geology*, 80, p. 412 – 431.

735 Guardado, L. R., L. A. P. Gamboa, and C. F. Lucchesi, 1989, Petroleum geology of
736 the Campos Basin, Brazil, a model for a producing Atlantic-type basin. *in* J. D. Edwards,
737 and P. A. Santogrossi, eds., *Divergent / Passive Margin Basins: AAPG Memoir 48*, p. 3-
738 79.

739 Guardado, L. R., A. R., Spadini, J. S. L Brandão, and M. R. Mello, 2000, Petroleum
740 System of the Campos Basin, *in* M. R. Mello and B. J. Katz, eds., *Petroleum Systems of*
741 *South Atlantic margins: AAPG Memoir 73*, p. 317-324.

742 Hessel M. H., and M. R. Mello, 1987, Caracterização das primeiras incursões
743 marinhas na bacia de campos caracterizadas por biomarcadores e bivalvios. *Anais do VI*
744 *Congresso Brasileiro de Geoquímica*, p. 484-487.

745 Hessel, M. H., 1993, Paleogeografia dos bivalvios da Formação Lagoa Feia,
746 Eocretáceo de Campos Simpósio de Geologia do sudeste, Rio de Janeiro, *Boletim de*
747 *Resumos e Breves Comunicações*. p. 22-23.

748 McKenzie, D. P., 1978, Some remarks on the development of sedimentary basins:
749 *Earth Planetary Sciences Letters*, v. 40, p. 25-32.

750 Muniz, M. C., 2013, Tectono-Stratigraphic evolution of the Barremian-Aptian
751 Continental Rift Carbonates in Southern Campos Basin, Brazil. PhD Thesis, Royal
752 Holloway University of London. 343 p.

753 Muniz, M. C., and D. W. J. Bosence, 2015, Pre-salt microbialites from the Campos
 754 Basin (offshore Brazil): image log facies, facies model and cyclicity in lacustrine
 755 carbonates. *in* D. W. J. Bosence, K. A. Gibbons, D. P. Le Heron, W. A. Morgan, T.
 756 Pritchard, and B. A. Vining, eds., *Microbial Carbonates in Space and Time: Implications for*
 757 *Global Exploration and Production*. Geological Society, London, Special Publications, 418,
 758 p. 221-242.

759 Platt, N. H., and V. P. Wright, 1991, Lacustrine carbonates: facies models, facies
 760 distributions and hydrocarbon aspects. *in* P. Anadón, L. Cabrera, and K. Kelts, eds.,
 761 *Lacustrine Facies Analysis*, International Association of Sedimentologists, Special
 762 Publication 13, p. 57-74.

763 Purser, B. H., P. Barrier, C. Montenat, F. Orszag-Sperber, P. Ott D'Estevou, J. C.
 764 Plaziat, and E. Philobos, 1998, Carbonate and siliciclastic sedimentation in an active
 765 tectonic setting: Miocene of the north- western Red Sea rift Egypt. *in* B. H. Purser, and D.
 766 W. J. Bosence, eds., *Sedimentation and Tectonics of Rift Basins: Red Sea–Gulf of Aden:*
 767 London, Chapman and Hall, p. 239-270.

768 Rangel, H. D., F. A. L. Martins, F. R. Esteves, and F. J. Feijó, 1994, Carta
 769 Estratigráfica da Bacia de Campos. *Boletim de Geociências da Petrobras*, v. 8, p. 203-
 770 217.

771 Rosendahl, B. R., D. J. Reynolds, P. M. Lorber, C. F. Burgess, J. McGill, D. L. Scott,
 772 J. J. Lambiase, and S. J. Derksen, 1986, Structural expressions of rifting: lessons from
 773 Lake Tanganyika, Africa. *in* L. E. Frostick, R. W. Renault, I. Reid, and J. J. Tiercelin, eds.,
 774 *Sedimentation in the African Rifts*. Geological Society London, Special Publication. 25, p.
 775 29-43.

776 Sadler, P.M., 1999, The influence of hiatuses on sediment accumulation rates:
 777 *GeoResearch Forum*, v. 5, p. 15-40.

778 Schaller, H., 1973, Estratigrafia da Bacia de Campos. *in* Anais do XXVII Congresso
779 Brasileiro de Geologia, v.3, p.247-258.

780 Schlager, W., 2005, Carbonate Sedimentology and Sequence Stratigraphy: SEPM
781 Concepts in Sedimentology and Palaeontology, 200 p.

782 Silva-Telles Jr., A. C., 1992, Novo Zoneamento das coquinas da formação lagoa
783 feia (Neojiquiá da Bacia de Campos) com base em ostracodes – aspectos evolutivos. *in*
784 Congresso Brasileiro de Geologia, 37., São Paulo, SP, Boletim de resumos expandidos, -
785 São Paulo: SBG, vol. 2, 489. p.

786 Silva-Telles Jr., A. C., 1996, Estratigrafia de sequências de alta resolução do
787 Membro Coqueiros da Formação Lagoa Feia (Barremiano / Aptiano da Bacia de Campos -
788 Brasil). Dissertação de Mestrado. Universidade Federal do Rio Grande do Sul. Curso de
789 Pós-graduação em Geociências Área de Concentração em Estratigrafia, 268p.

790 Soreghan, M. J., and A. S. Cohen, 1996, Textural and compositional variability
791 across littoral segments of Lake Tanganyika: The effect of asymmetric basin structure on
792 sedimentation in large rift lakes. AAPG Bulletin, v. 80, p. 382-409.

793 Talbot, M. R., 1990, A review of the palaeohydrological interpretation of carbon and
794 oxygen isotopic ratios in primary lacustrine carbonates: Chemical Geology, v. 80, p. 261-
795 279.

796 Thompson, D. L., J. D Stilwell, and M. Hall, 2015, Lacustrine carbonate reservoirs
797 from Early Cretaceous rift lakes of Western Gondwana: Pre-Salt coquinas of Brazil and
798 West Africa: Gondwana Research, v. 28, p. 26–51.

799 Winter, W. R., R. J. Jahnert, and A. B. França, 2007, Carta Estratigráfica da Bacia
800 de Campos, Boletim de Geociências da Petrobras, Rio de Janeiro, v. 15, p. 511-529.

801 Wilson, M. E., 2002, Cenozoic carbonates in Southeast Asia: implications for
802 equatorial carbonate development. Sedimentary Geology. v.147, p. 295-328.

803 Wright, V. P., 1990, Singenetic formation of grainstones and pisolites from fenestral
804 carbonates in peritidal settings – discussion. *Journal of Sedimentary Petrology*, 60: p. 309-
805 310.

806 Wright, V. P., 2012, Lacustrine carbonates in rift settings. *in* J., Garland, J. E.
807 Neilson, S. E. Laubach, and K. J. Whidden, eds., *Advances in Carbonate Exploration and*
808 *Reservoir Analysis*: Geological Society, London, Special Publication, 370, p. 39-47.

809 Wright, V. P., and A. J. Barnett, 2015, An abiotic model for the development of
810 textures in some South Atlantic early Cretaceous lacustrine carbonates. *in* D. W. J.,
811 Bosence, K. A. Gibbons, D. P. Le Heron, W. A. Morgan, T. Pritchard, B. A. Vining, eds.,
812 *Microbial Carbonates in Space and Time: Implications for Global Exploration and*
813 *Production*: Geological Society, London, Special Publications, 418, p. 209-219.

814

815 **FIGURE HEADINGS**

816 **Figure 1.** Location map with the main oil fields (in yellow) in the Campos Basin – Red rectangle delineates
817 the area of this study. Orange colors are carbonate hosted oil fields (Courtesy Petrobras).

818 **Figure 2.** Summary of the chrono- and lithostratigraphic divisions of the Lower Cretaceous of the Campos
819 Basin together with tectono-stratigraphic phases of basin evolution. The carbonate rocks of the Coqueiros
820 Formation are the subject of this study (After Winter *et al.*, 2007).

821 **Figure 3 -** Seismic horizons mapped in this study exemplified by profile from well 20. Lithologies and phases
822 of basin evolution also indicated.

823 **Figure 4.** NW to SE seismic section in time indicating units mapped within the southern Campos Basin (red-
824 acoustic basement and volcanics, dark blue-top Atafona and base Coqueiros, light blue- top Coqueiros, dark
825 pink-base salt, purple-top salt). Inset shows top basement surface within study area and approximate
826 location of seismic line.

827 **Figure 5.** 3D view of study area (see Figure 1) in Geoprobe of top acoustic basement surface in TWT
828 illustrating 3 main structural domains described in text and location of wells.

829 **Figure 6.** Stratigraphic cross section: proximal to distal well ties through the study area indicating electrical
830 logs, core coverage, phases of basin evolution and unconformities mapped. Section flattened to base salt.

831 **Figure 7.** Core slabs (with 1 cm scales) and photomicrographs (1mm scales) of rocks described in Table I.
832 A, E) Brecciated Mudstone (Bk) interpreted as exposure surface. Younger material fills the interstitial clast
833 space.. In core slab A breccia is overlain by a thin bed of laminated siltstone (ST). B, F) Bivalve Rudstone
834 (Rt) with interbedded coarse terrigenous sand. C, G) Bivalve rudstone (Rc) articulated and disarticulated
835 (whole and broken) shells with interparticle porosity and clean grainstone matrix. D,H) Bivalve Rudstone
836 (Rm) with muddy matrix and disarticulated bivalves. I) Core slab of oncoid rudstone (Rm). J) Core slab of
837 muddy rudstone with articulated bivalves, some in upright in situ position. K) Marl erosively overlain by a 10
838 cm thick bed of rudstone, interpreted as a tempestite. L) Mudstone (MD) with irregular bedding, dark and
839 organic rich.

840 **Figure 8.** Facies model. Proximal to distal lake margin illustrating interpreted facies distribution in relation to
841 lake level and fair weather (FWWB) and storm (SWB) wave base.

842 **Figure 9** Gamma log, thin-sections from sidewall cores and BHI logs from Coqueiros and Macabu Fm in well
843 20 (located in Figure 1). BHI log indicates plane bedding, coarse grainy texture and curved conductive
844 shapes (interpreted as bivalve shells). Side wall core thin-sections 1) ostracod –rich grainstone with
845 stevensite (brown), (2-3) show clean bivalve and gastropod rudstones with disarticulated, neomorphosed,
846 thick-shelled molluscan shells with good interparticle porosity, 4) digitate stromatolite (microbialite) from
847 Macabu Fm.

848 **Figure 10.** Schematic 3-D diagram of the Barremian Lagoa Feia lake indicating depositional environments
849 and occurrences of the 4 facies associations identified based on cores and logs (mod. from Platt & Wright
850 1991).

851 **Figure 11.** Graphic log and Gamma log from cored interval in well 7 (for location see Figure 6) illustrating
852 five meter-scale cycles within the Lacustrine Carbonate Platform Facies Association. Each cycle is bounded
853 by a brecciated and /or Fe-stained surface (facies Bk), or with associated clastics and gamma peaks. The
854 two thicker cycles show cleaning up gamma trends tied to coarsening facies trends from packstones and
855 grainstones to thick rudstone units.

856 **Figure 12.** Tectono stratigraphic model. a) Seismic section and flattened on base salt showing the main
857 structural features and the key surfaces mapped. For location see Figure 5b) Interpreted section showing the
858 3 identified domains and the stratigraphic geometries of each sub-basin fill for each domain. c) Sketches to
859 indicate structural template, stratigraphic geometries and carbonate platform morphologies interpreted from
860 3D seismic.

861 **Figure 13.** Block diagram showing the structural setting, facies associations and depositional environments
862 for mixed siliciclastic – carbonate sediments of Domain I. Based on wells 1-12 and seismic data.

863 **Figure 14.** Block diagram of Domain II tectono-stratigraphic model. Carbonate platform forming on an
864 accommodation zone (horst block) with an aggradational build-up and basinward progradation. Model based
865 on 3D seismic interpretation, sidewall core analysis and BHI interpretation in the well 20. The green colored
866 facies on the eastern margin of the model is a deep lake facies and it is thought this fault bound area area

867 may have undergone inversion from originally deeper water areas.

868 **Figure 15.** Block diagram showing a Domain III isolated carbonate platform. In this tectonic context, a
869 carbonate platform is formed over the relict horst, showing progradation of the platform margins that are
870 subsequently onlapped by deeper water sediments. This model is based purely on seismic interpretations
871 with ties to nearby cored horizons within the southern Campos Basin.

872 **Table 1** Description and interpretation of core-based facies from the Lagoa Feia Gp.

873

874 MOISES CALAZANS MUNIZ - *Petrobras, Av. República do Chile, 330, 17° andar, Centro,*
875 *CEP:20031-170, 17°, Rio de Janeiro, RJ, Brazil; mcalazans@petrobras.com.br*

876 Moises C. Muniz is Senior Geologist, consultant, with vast experience in exploration works
877 focused on tectonostratigraphy, seismicstratigraphy, facies and sequence stratigraphy
878 analysis applied to Cretaceous carbonate platforms of the southeast Brazilian basins. He
879 received his Ph.D. at Royal Holloway University of London in 2012.

880

881 DAN BOSENCE - *Department of Earth Sciences, Royal Holloway University of London,*
882 *Egham, Surrey, TW200EX, UK; d.bosence@es.rhul.ac.uk*

883 Dan Bosence is Emeritus Professor of Carbonate Sedimentology with extensive
884 experience of modern and ancient carbonate sediments. His research focus is on facies
885 and sequence stratigraphic analysis, high-frequency cycles, and tectonic controls on
886 carbonate platforms. He divides his time between university-based research, training and
887 consultancy.

Figure 1

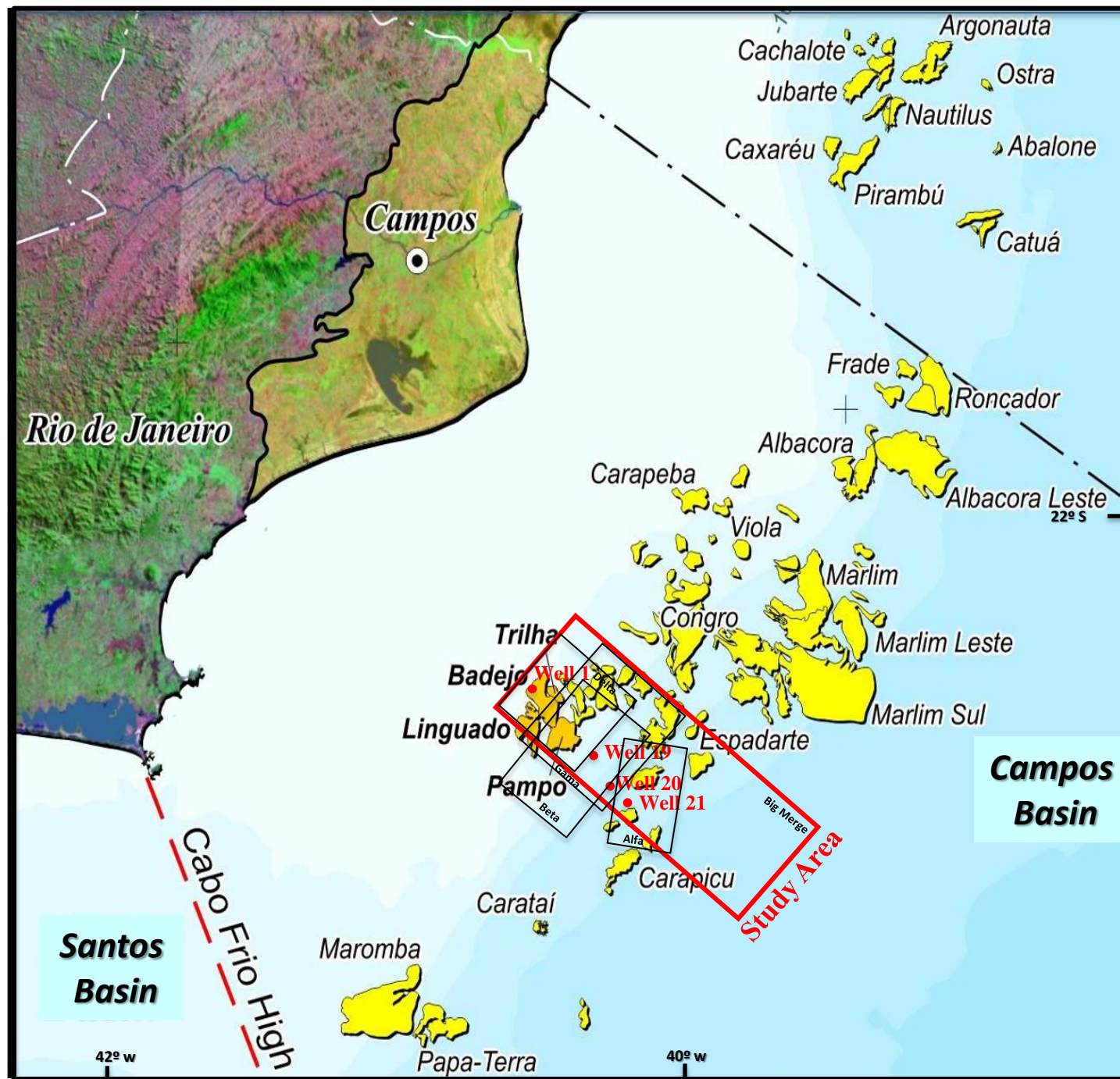
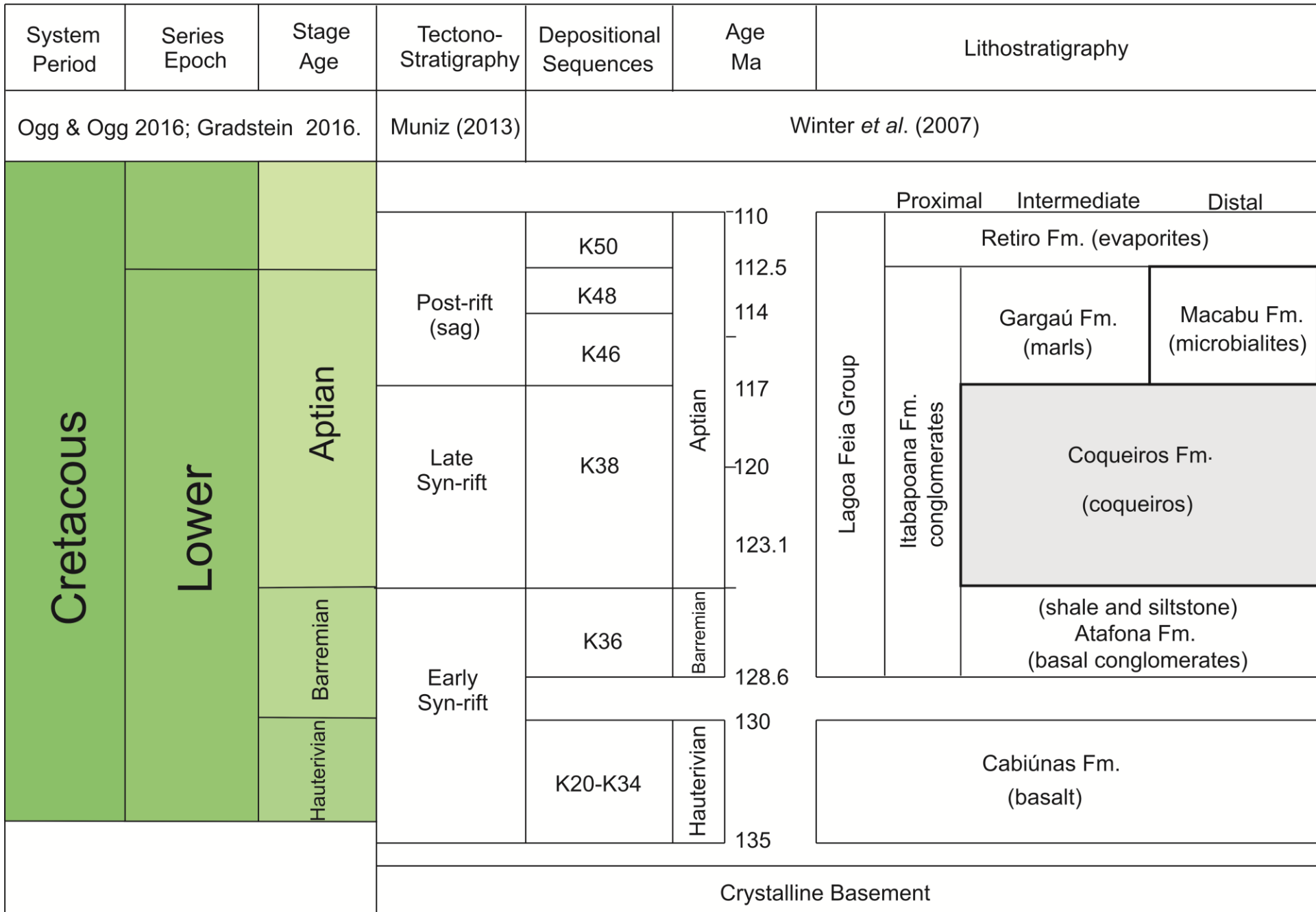


Figure 2



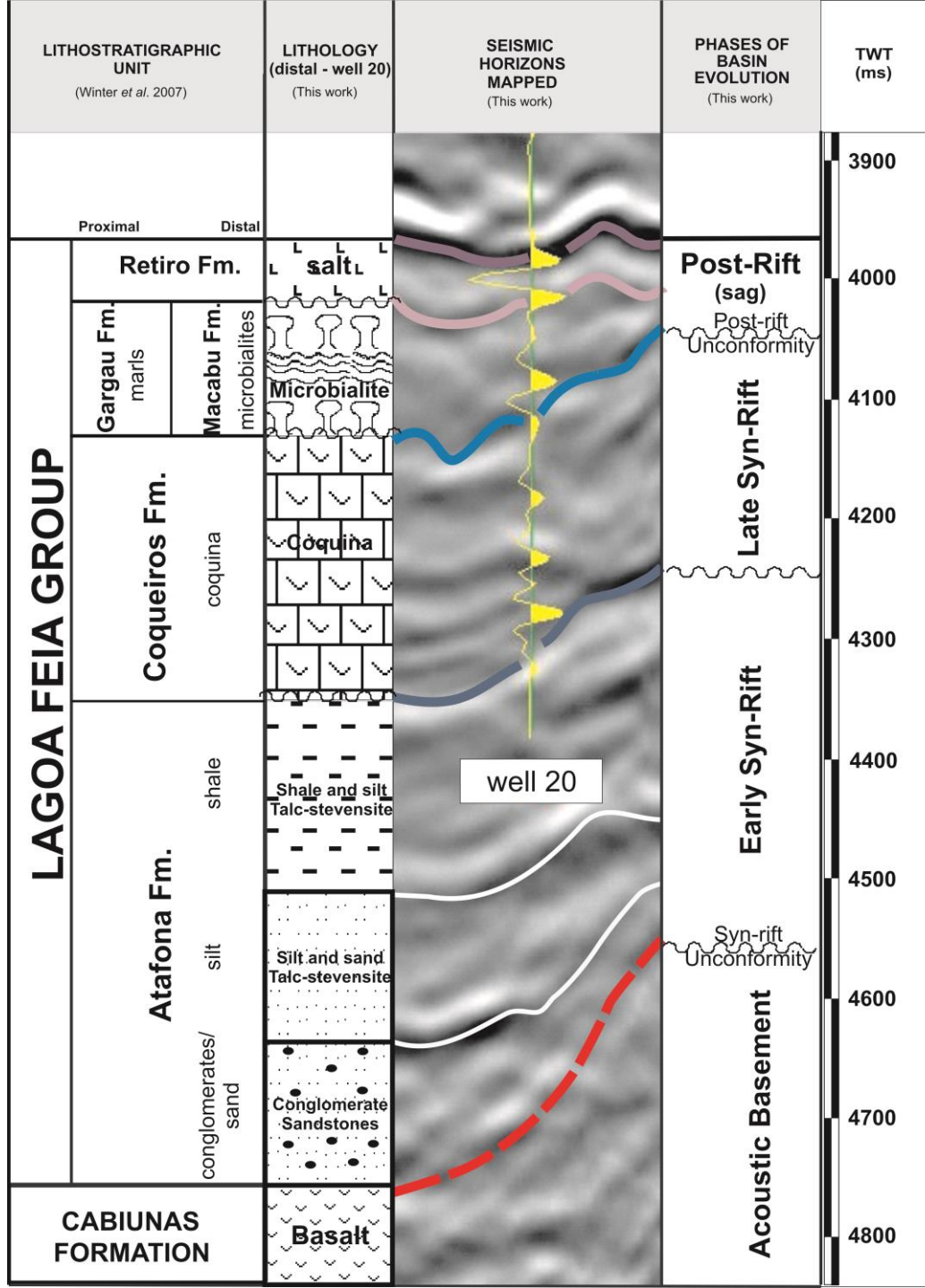


Figure 3

Figure 4

Seismic Section Dip (time)

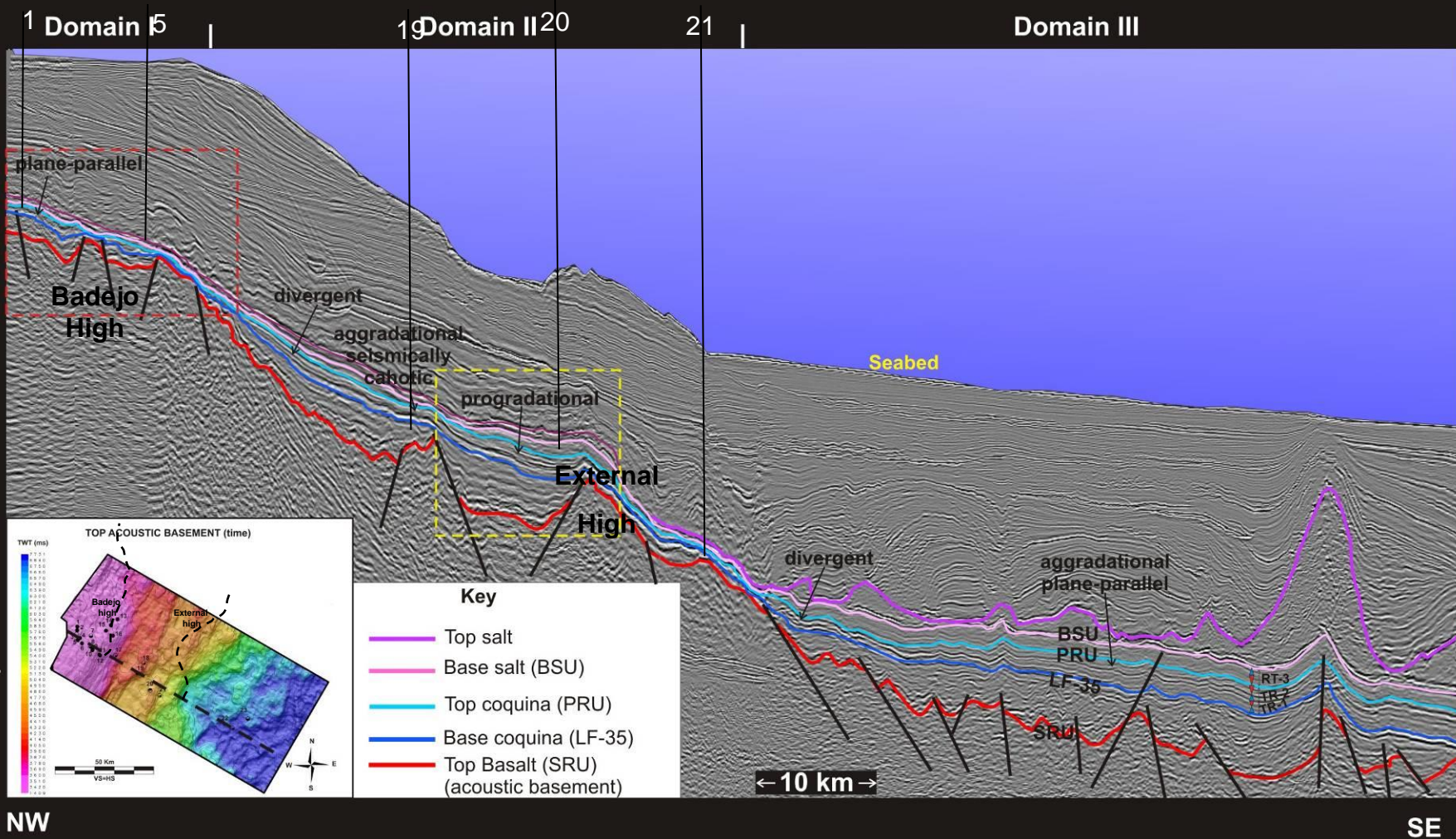


Figure 5

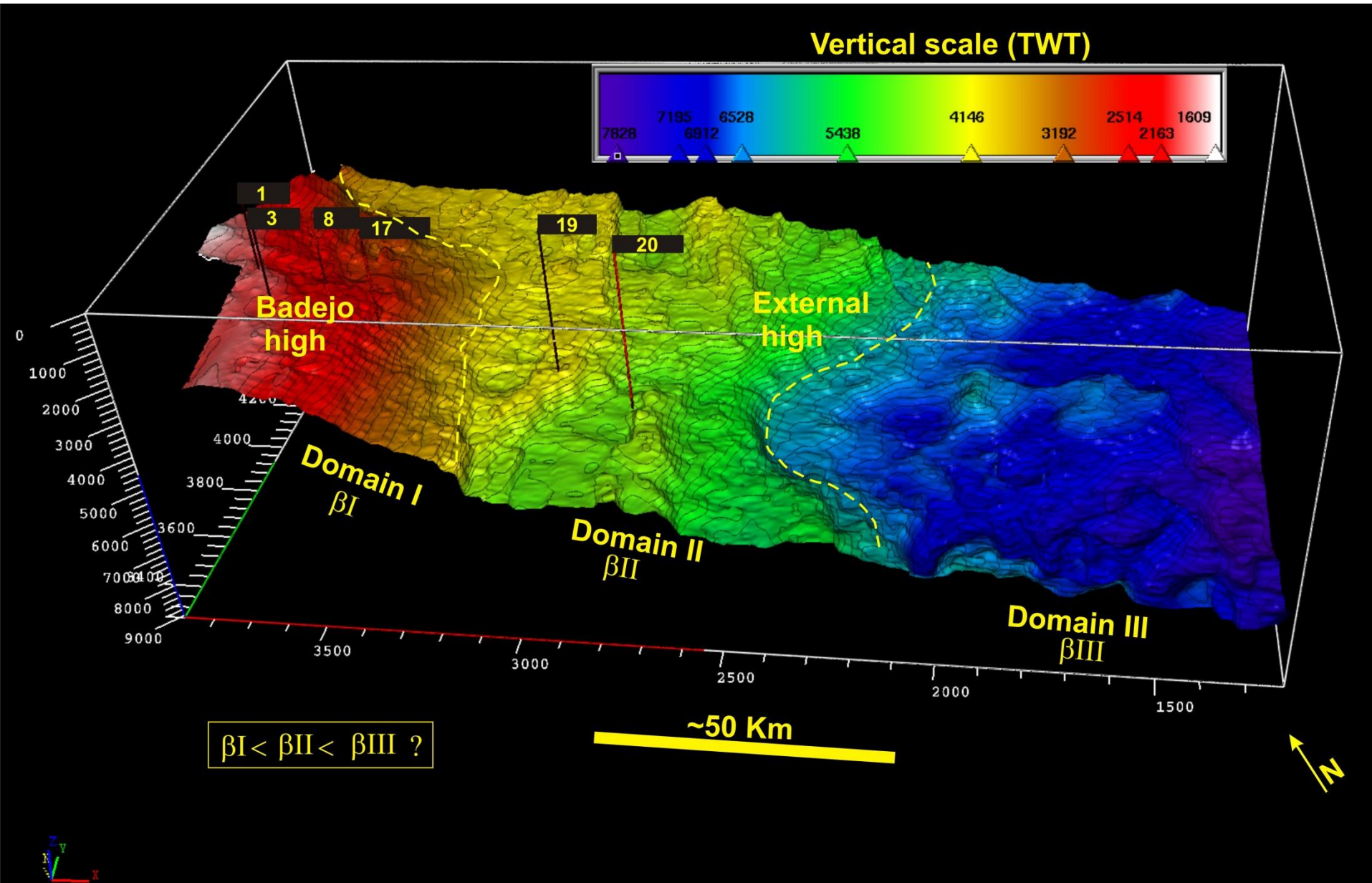


Figure 6

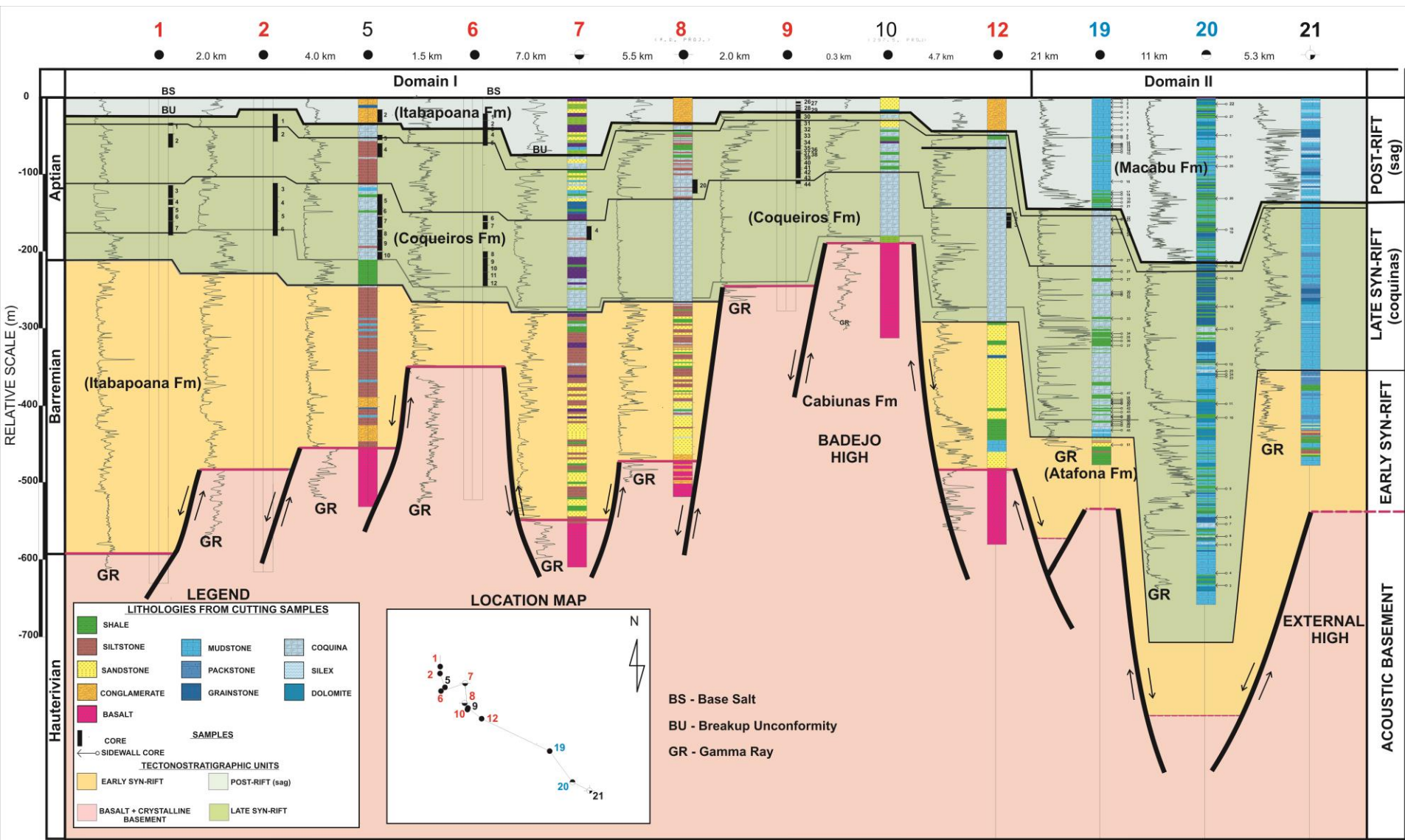


Figure 7

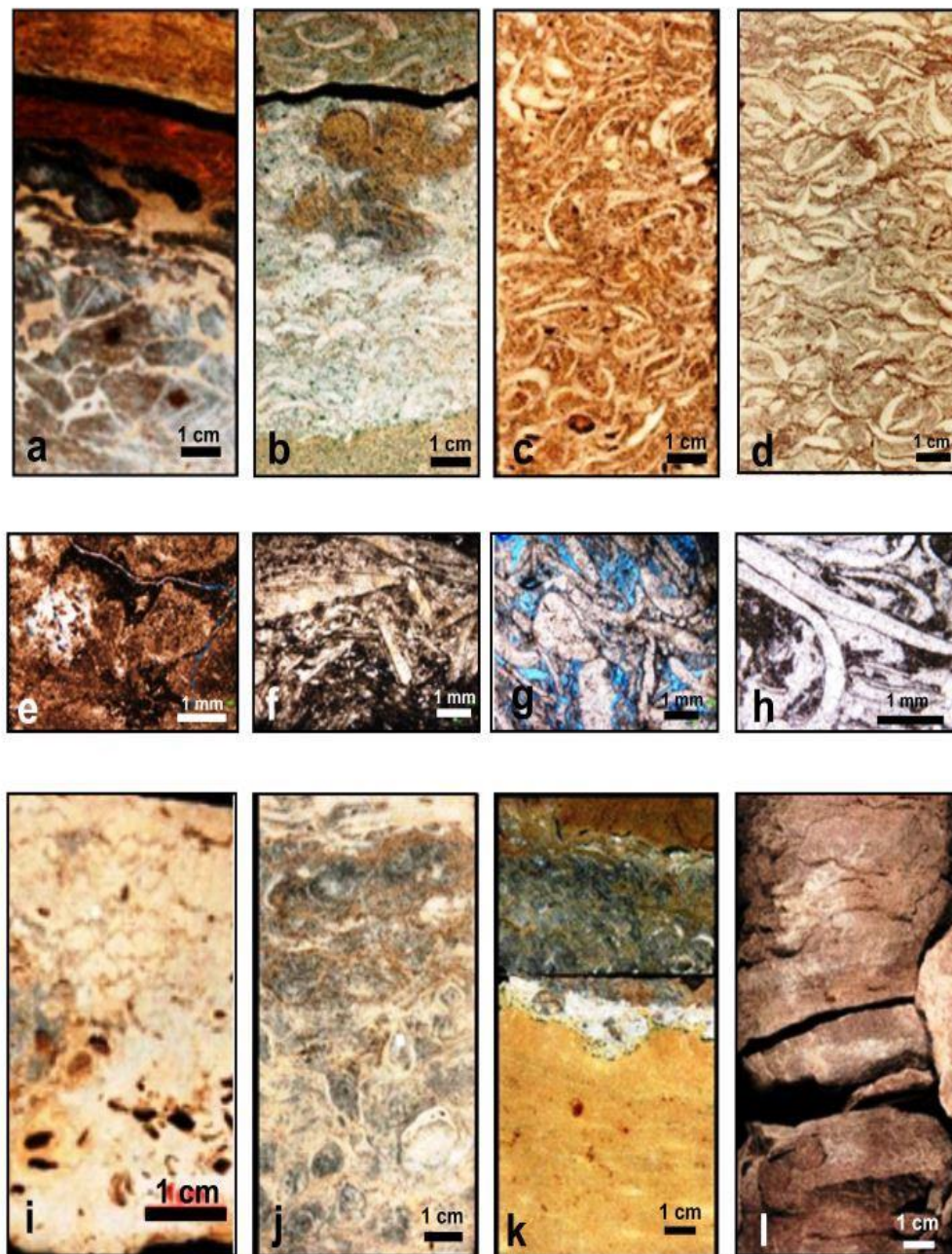
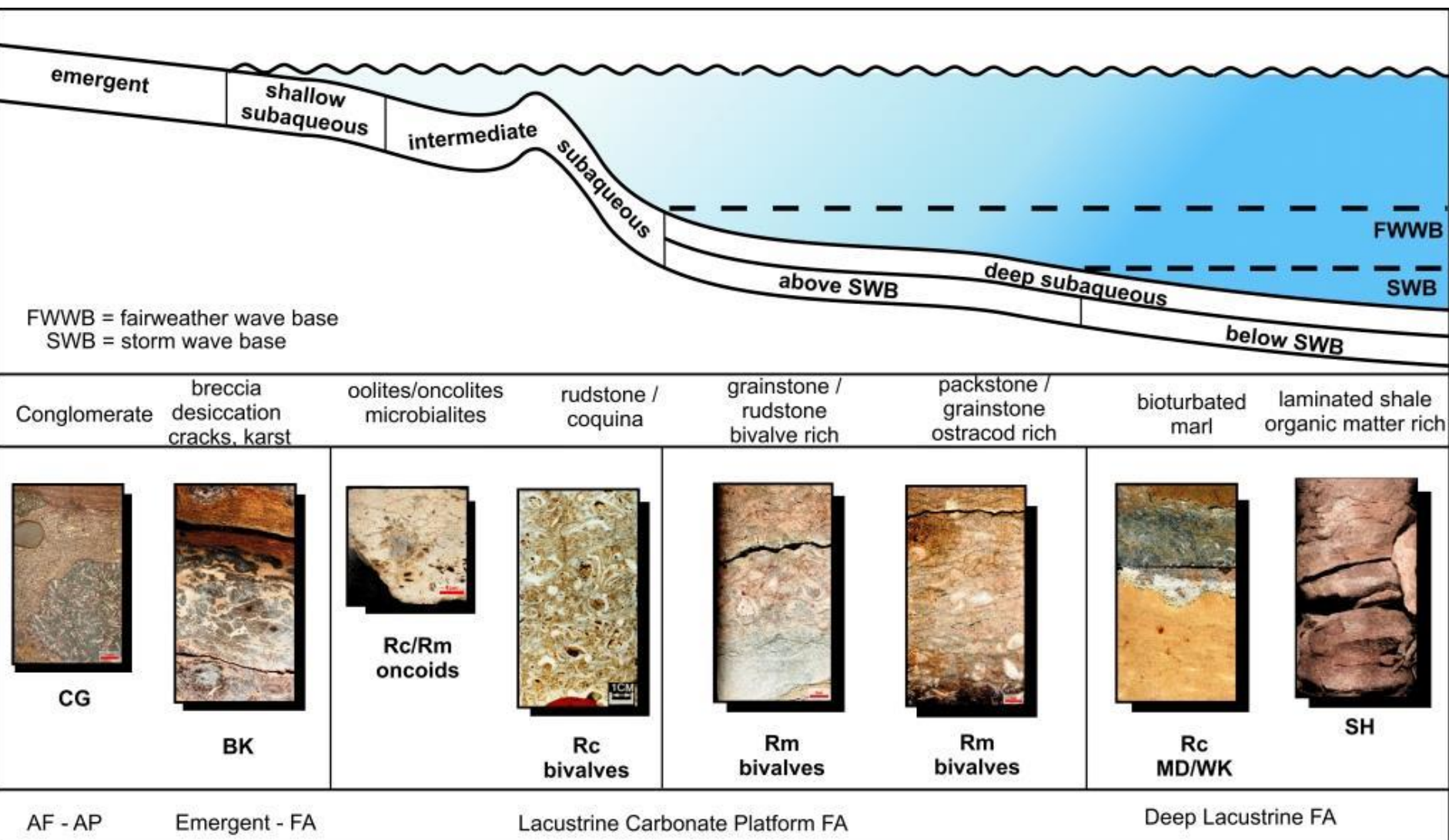
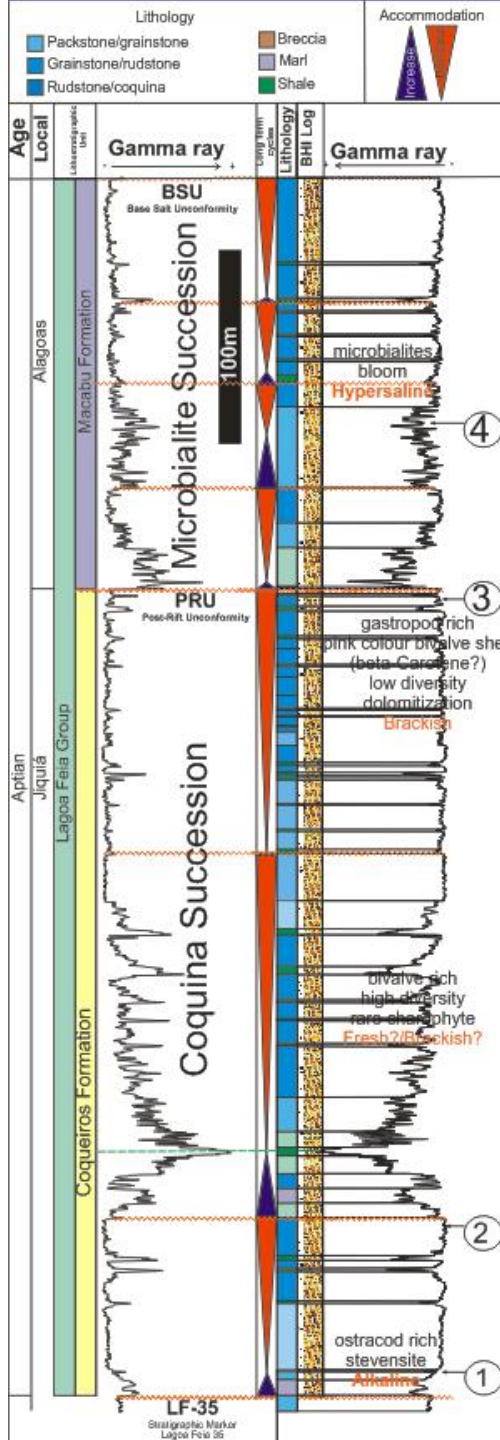


Figure 8





Well 20

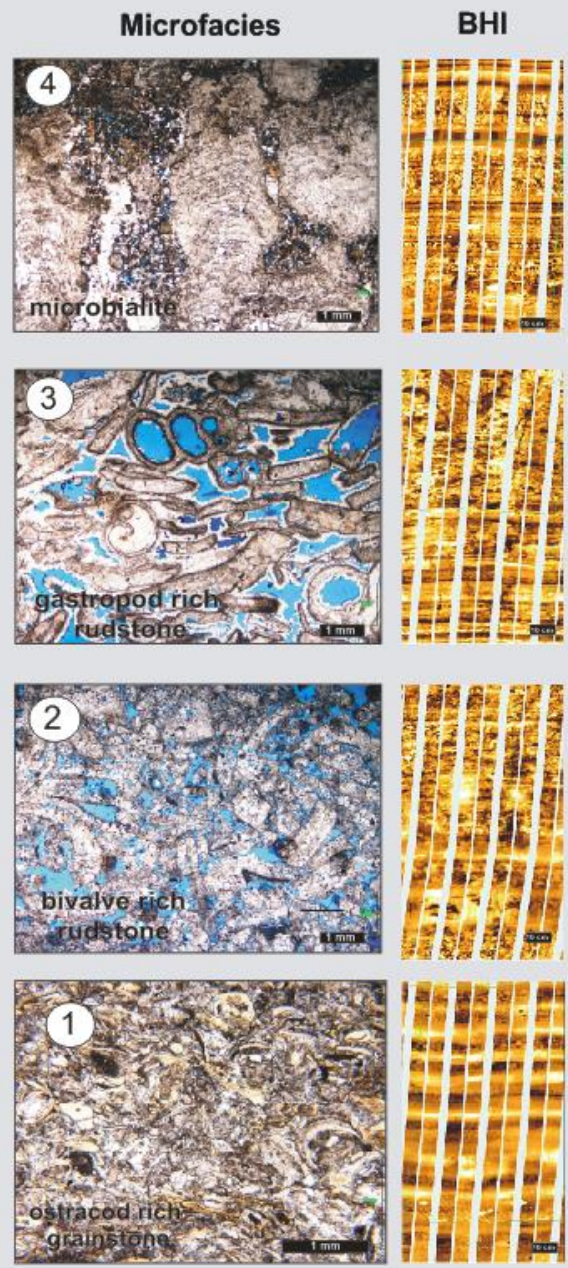
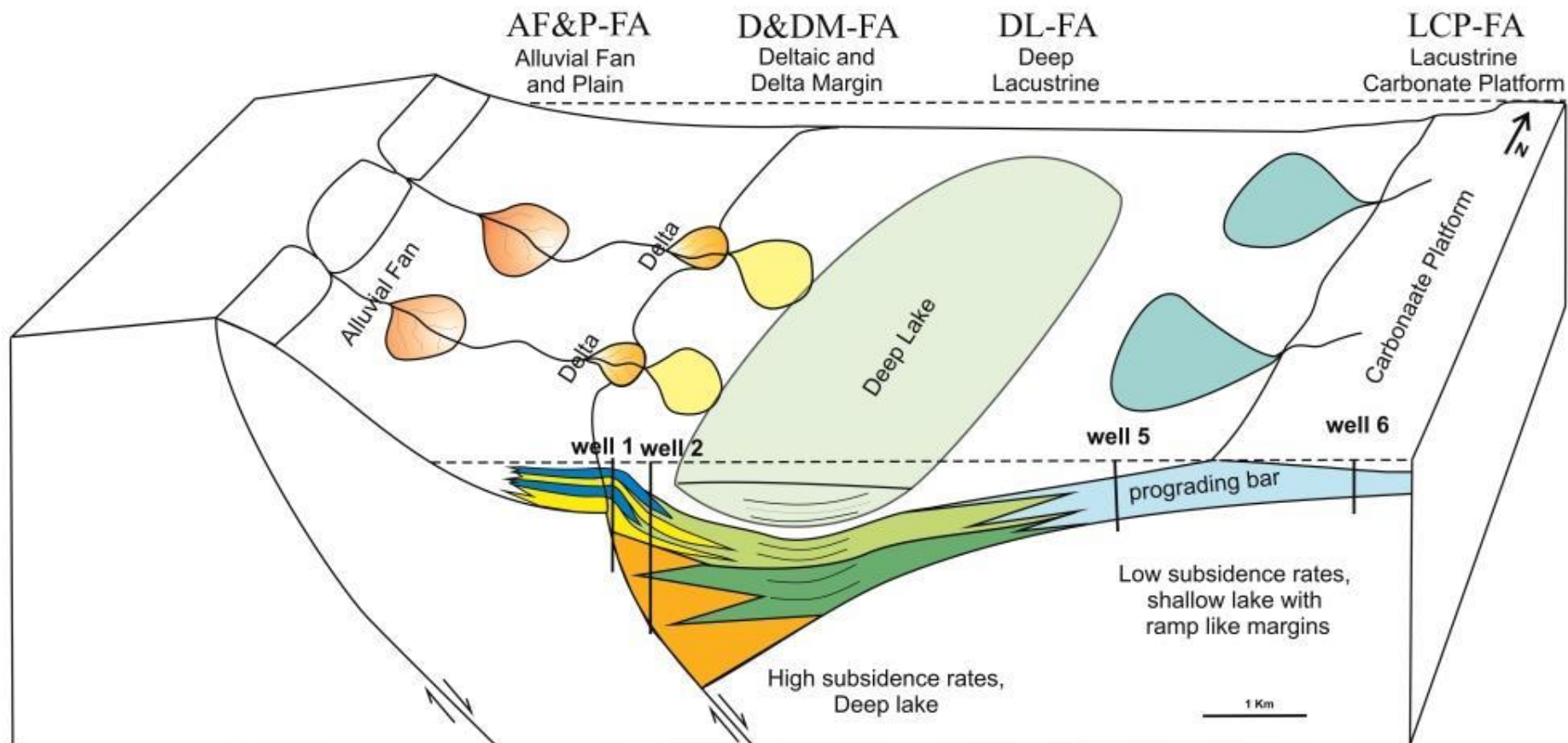
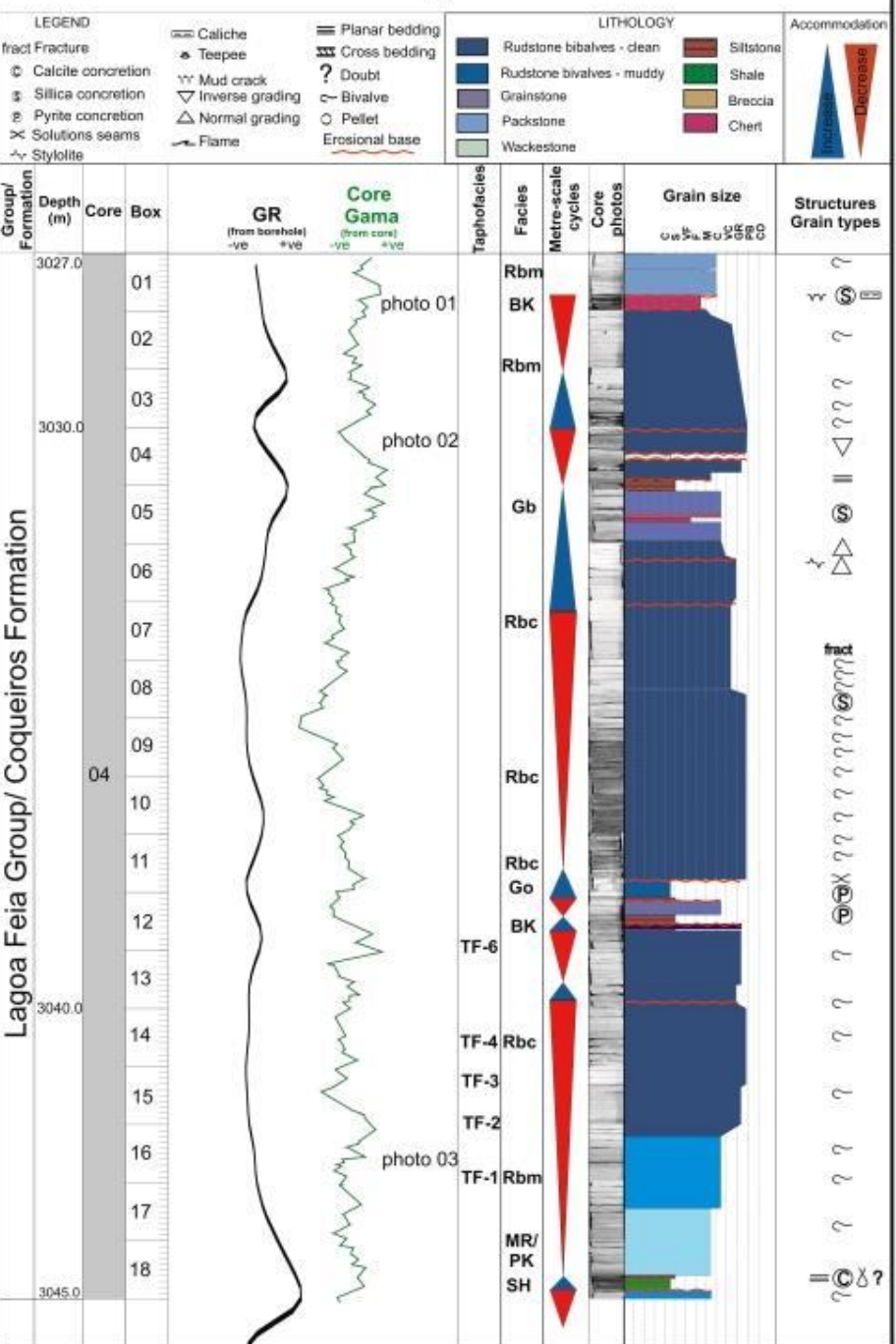


Figure 9

Figure 10



Core Analysis



Well 7 Core 04

Figure 11

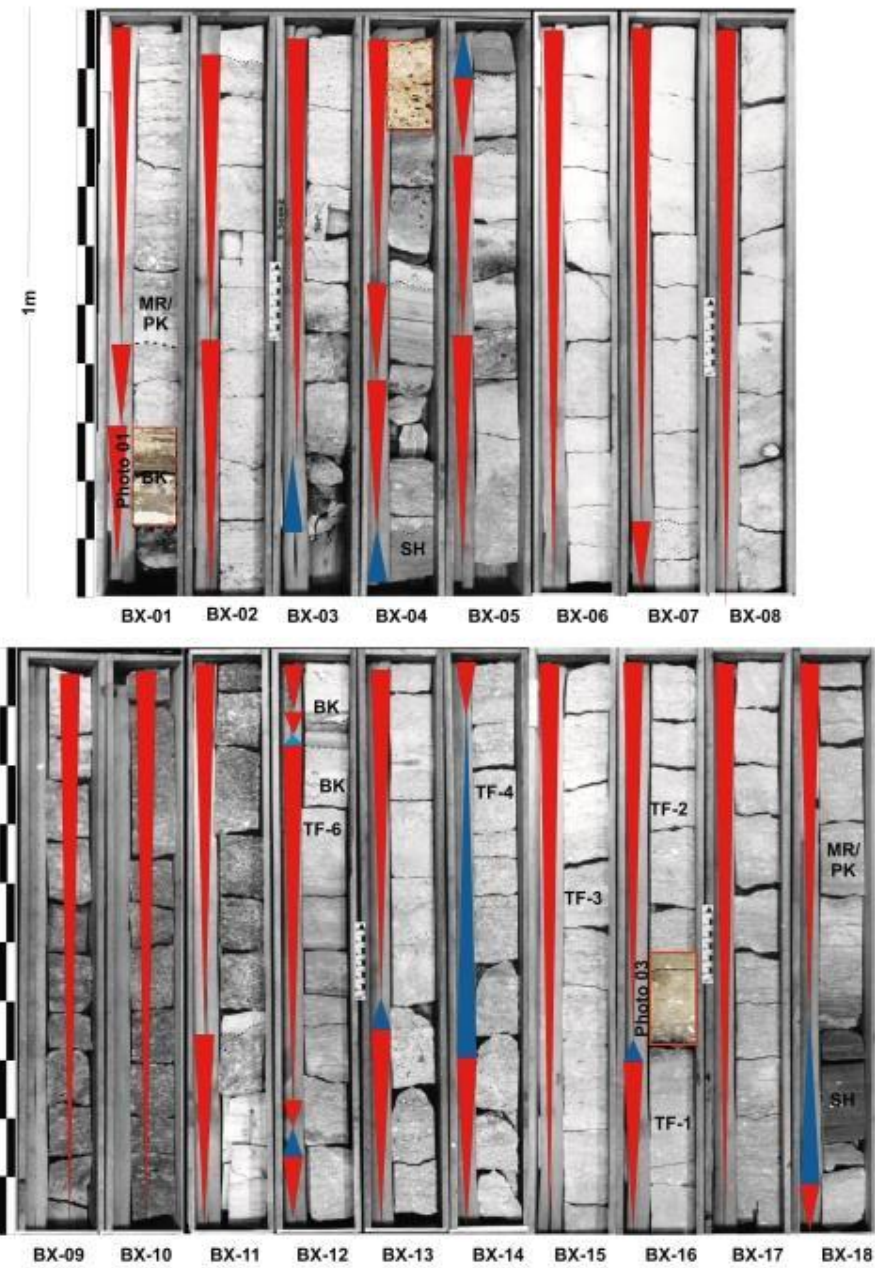


Figure 12

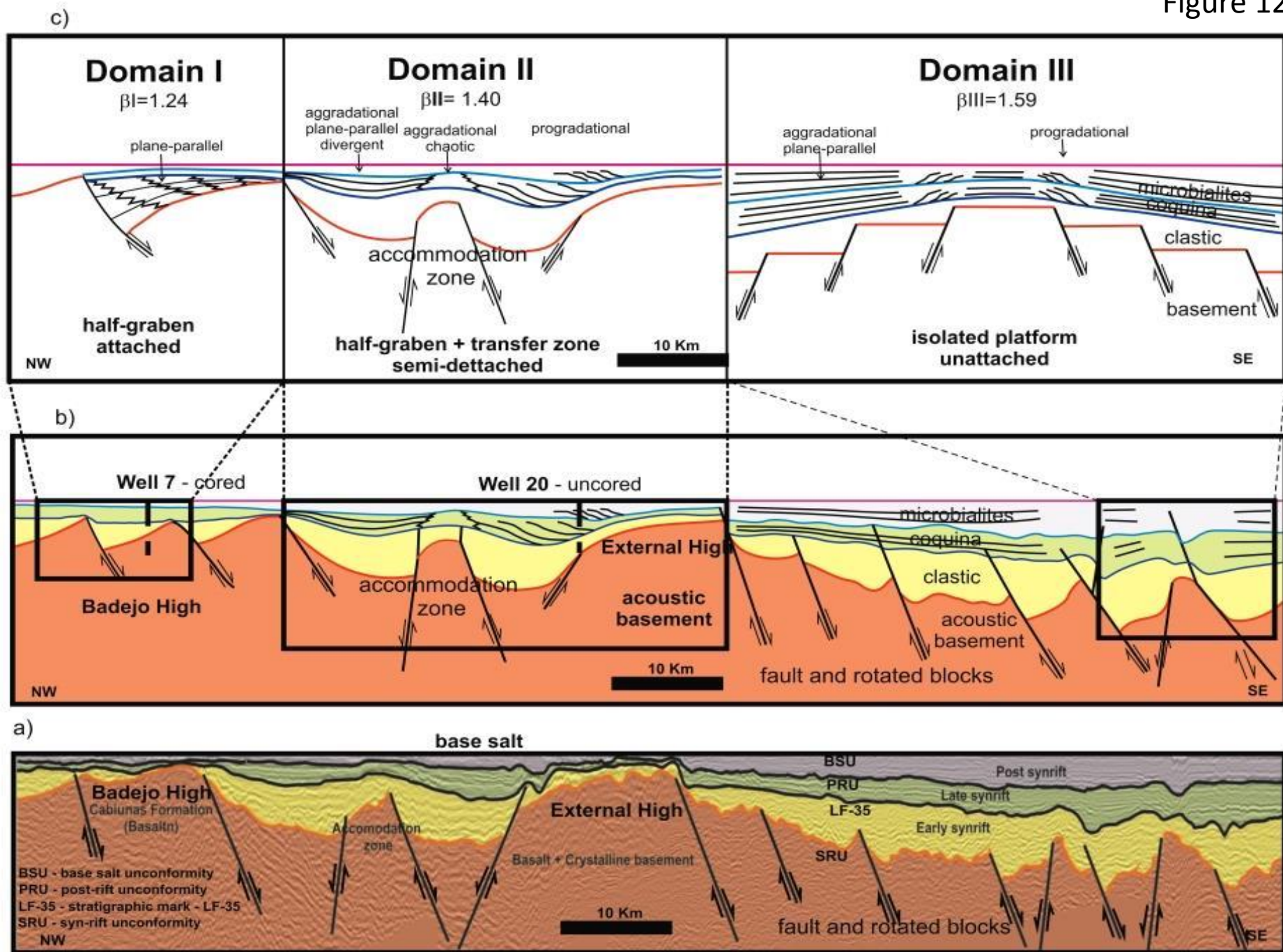


Figure 13

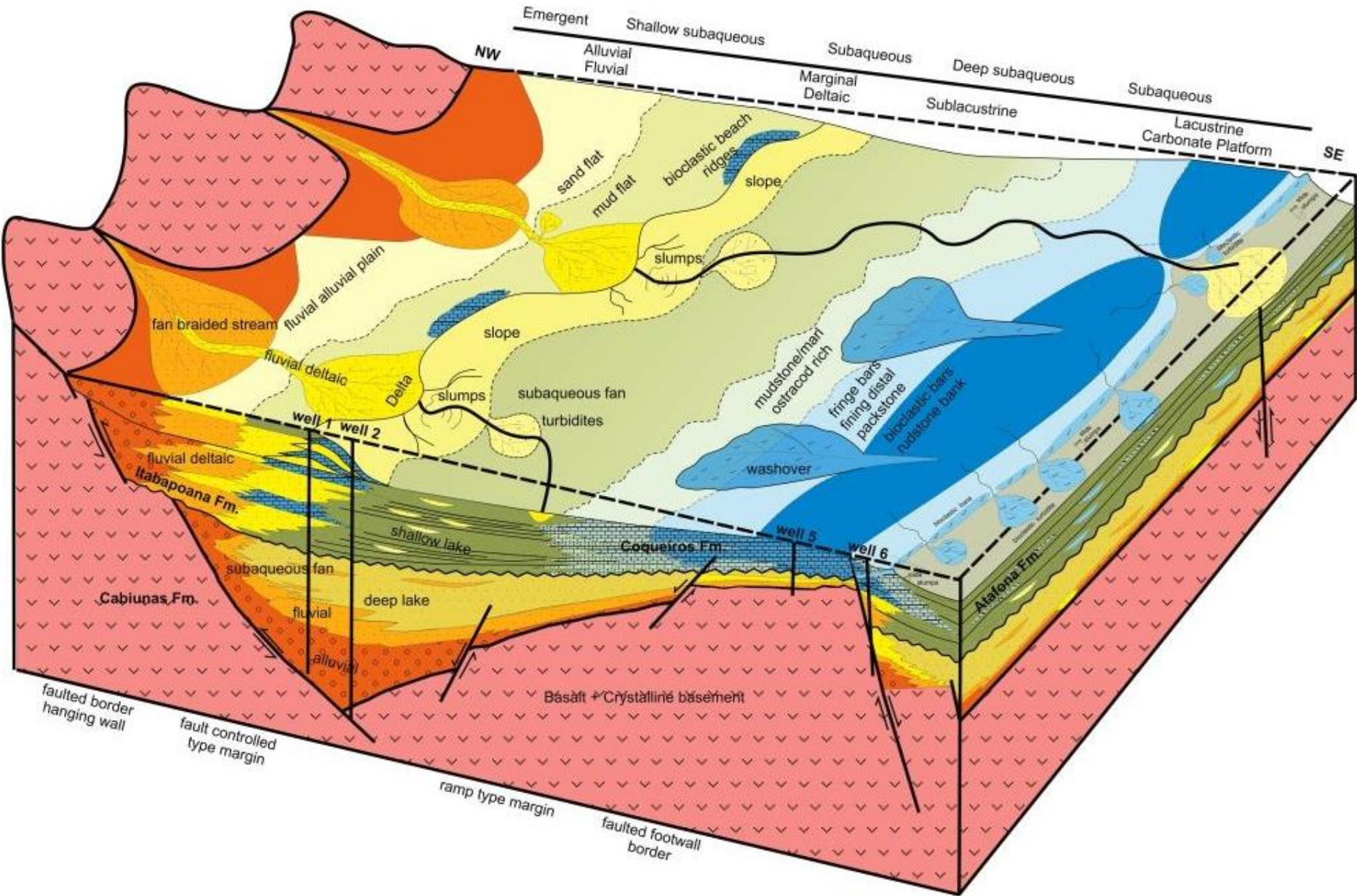


Figure 14

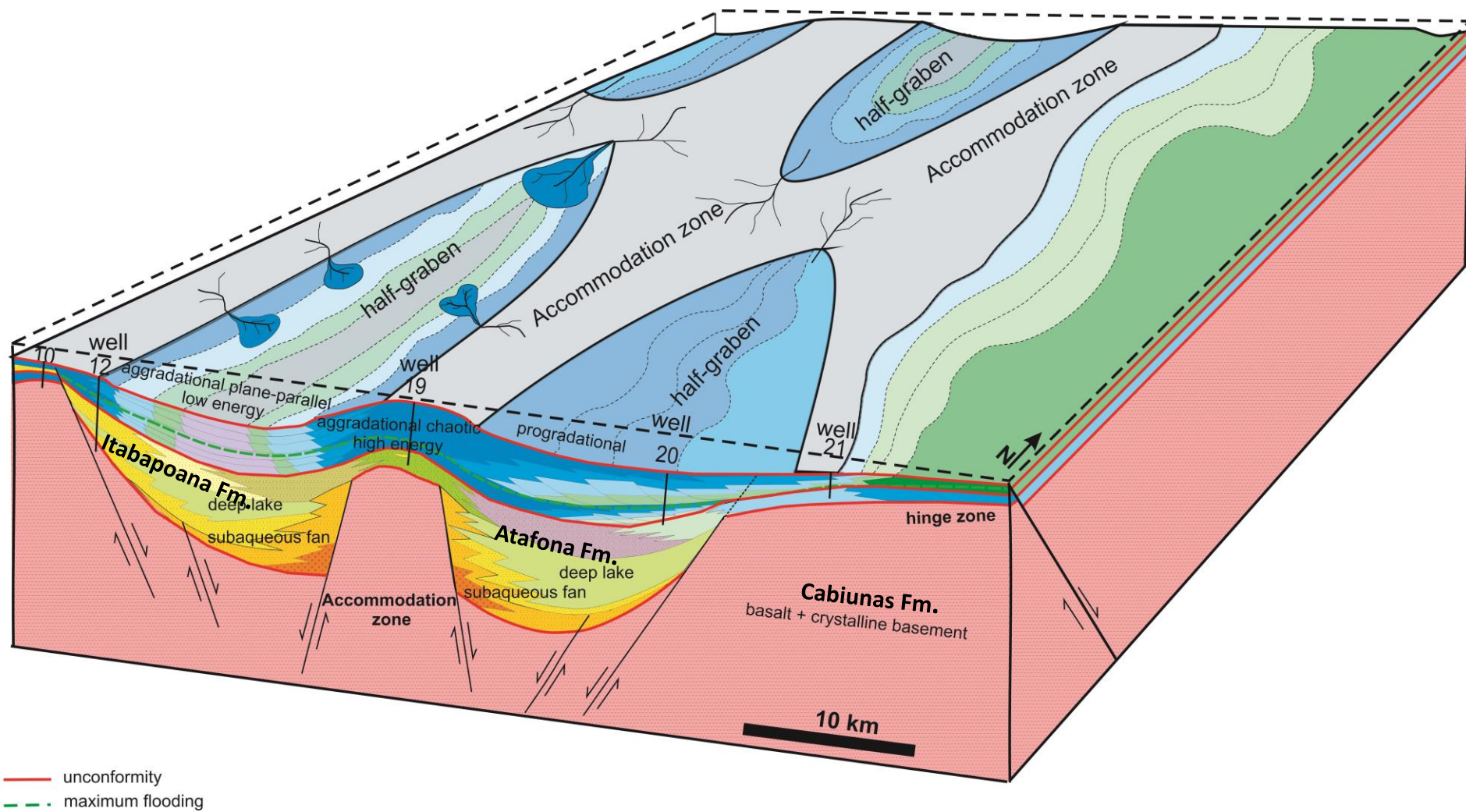
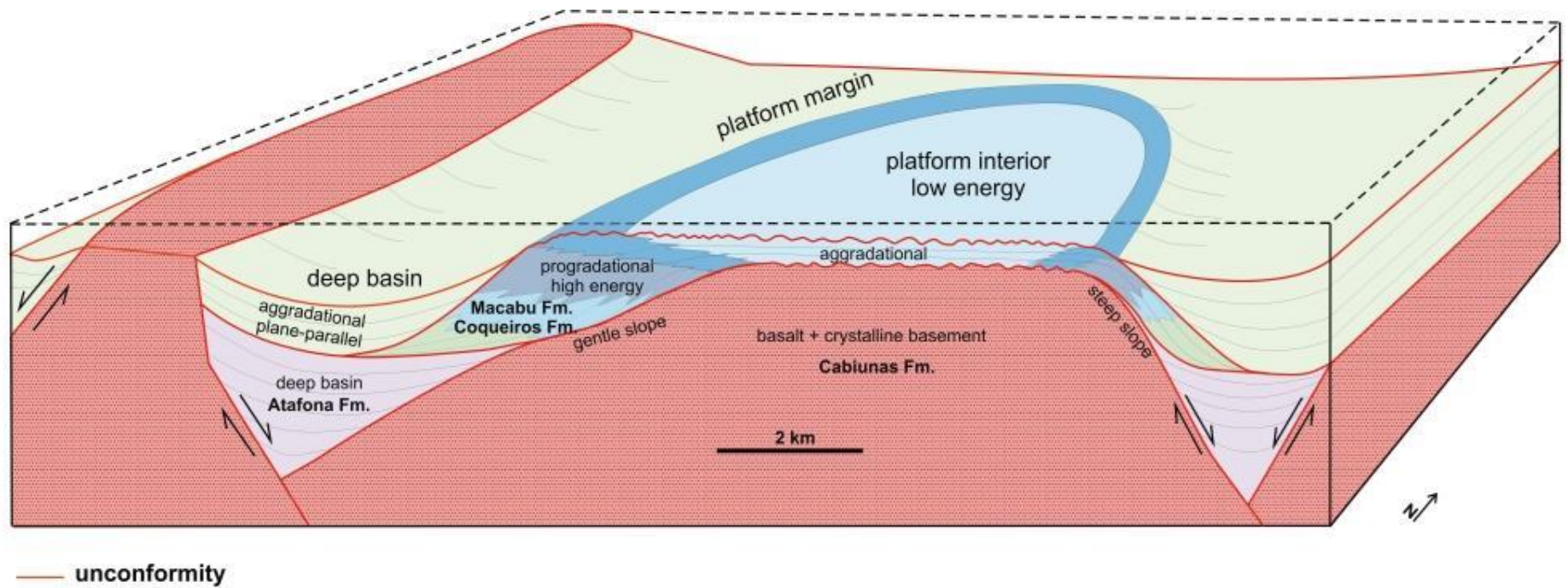


Figure 15



Carbonate facies	Structures	Textures	Composition	Diagenetic Features	Porosity Types	Depositional Processes
Mudstone MD	10-30 cm beds	mudstone	Peloids <10% bivalve and ostracod frags. Locally argillaceous	Localised pyrite, phosphate & calcite concretions Microspar	Fracture	Abiotic precipitation/ abrasion/disintegration of skeletal material Quiet water Deep subaqueous, dysoxic
Marl ML	Lamination	Bioturbation	Mixed carbonate and terrigenous mud Ostracod fragments			Quiet water, deep subaqueous, dysoxic-oxic
Wackestone WK	Centimetric to m-thick massive beds Local erosive contacts	Matrix support Bioturbation	Bivalves, ostracods rare gastropods Peloids, Stevensite, volcanic lithoclasts	Local silica nodules and brecciation	Fracture	Quiet water Deep or protected subaqueous
Packstone P	Centimetric to m-thick massive beds w. erosive contacts. Rare low L x-stratification	Aligned shells Normal grading Local bioturbation	Bivalves, ostracods gastropods Peloids, Stevensite, volcanic lithoclasts	Solution seams, stylolite Replaced & recrystallised shells Spar cement Microspar matrix	Vuggy Mouldic Fracture	Erosively based graded beds- storm events and density currents. Matrix infiltrated grainstones
Grainstone G	Thin – thick beds stacked up to 3 m X-stratification	Fine-coarse grain supported Moderate-well sorted Subrounded	Bivalves (whole or broken), gastropods, ostracods Peloids, ooids Quartz, volcanic lithoclasts	Replaced & recrystallised shells Spar cement Locally silicified Dissolution seams stylolites	Interparticle mouldic vuggy Micro-fractures	Subaqueous high-energy, mud free waters Above fair weather wave base
Floatstone	Up to 1 m thick	Skeletal frags floating in silt to	Bivalves (articulated or disarticulated),	Replaced & recrystallised shells	Fracture	Quiet water Deep or protected

F		sand size matrix	gastropods, ostracods Rare oncoids	Microspar matrix Stylolites		subaqueous Bivalve colonization and local reworking
Rudstone muddy Rm	Cm to m-thick beds Bioturbation	Inverse graded beds Skeletal frags with peloidal muddy matrix	Bivalves (disarticulated or articulated) <3 cm <i>Trigonodus</i> , <i>Kobayashites</i> , <i>Camposella</i> , Stevensite Oncoids	Replaced & recrystallised shells Microspar and spar cement Local silicification, stylolites		Subaqueous moderate-energy waters Above fair weather wave base Intermediate subaqueous lake
Rudstone sandy Rt	Cm to m-thick beds	Skeletal frags in matrix in coarse terrigenous sand	Disarticulated and fragmented <i>Camposella</i> Lithoclasts (volcanic) feldspar quartz	Recrystallised/replaced & silicified shells Spar cement Local stylolites	Interparticle	Proximal environments Subaqueous high-energy, Above fair weather wave base Intermediate subaqueous lake
Rudstone clean Rc	Cm to m-thick shell beds & X beds Bed parallel alignment, concave-down or -down	Well rounded bivalve frags (<5 cm) in grainstone	Unionid bivalves <i>Trigonodus</i> , <i>Camposella</i> , <i>Desertella</i> and fragments Oncoids	Replaced & recrystallised shells Spar cement Local silicification, stylolites	Interparticle mouldic vuggy	Subaqueous high-energy, mud free waters Above fair weather wave base Intermediate subaqueous lake
Siliciclastic Facies	Structures	Textures	Composition	Diagenetic Features	Porosity Types	Depositional Processes

Shale SH	Laminated, syn-sedimentary folds. Locally brecciated Microbial laminite	Clay and silt size	Quartz and mica. Locally bioclast rich (bivalves, ostracods & fish)	Calcite nodules Pyrite	None visible	Deep subaqueous lake or delta plain. Lack of bioturbation and reduced biota implies low oxygen
Siltstone ST	to 0.3 m thick beds Up to 7 m thick when stacked Weak laminae	Bioturbation and mottling	Clay minerals, mica, quartz, volc rock frags, mud pebbles Abraded mollusc bioclasts, fish bones	Calcite and pyrite nodules Spar cement Fractures	None visible	Quiet water deposition Burrowing indicates oxic zone Deep subaqueous or protected shallow lacustrine waters
Sandstone fine Sf	0.1 to 1m thick beds stacked to 6 m units Low angle X beds Ripple lamination Erosive bases	Very fine to fine sand Locally argillaceous Fluidisation	Quartz, feldspar, mica, volc rock frags, Clay minerals, Abraded mollusc bioclasts, fish bones	Calcite and pyrite nodules Replaced & recrystallised shells Spar cement Fractures	None visible	Fluvio-deltaic settings with moderate energy Proximal lacustrine margins
Sandstone medium Sm	Centri-metric beds plane laminated X- bedded Fluidisation structures	Medium sand Bioturbation	Quartz, feldspar, mica, volc rock frags, garnet, , Abraded mollusc bioclasts,	Replaced & recrystallised shells Spar cement Local silicification	Interparticle	Fluvio-deltaic settings with moderate energy Proximal lacustrine margins Lacustrine fans
Sandstone coarse Sc	Centri-metric thick beds Plane laminated X- bedded Graded beds	Coarse sand	Quartz, feldspar, mica, volc rock frags Bivalve frags <4 cm	Replaced & recrystallised shells Spar cement Local silicification	Interparticle	Fluvio-deltaic settings with moderate-high energy Proximal lacustrine margins Lacustrine turbidite fans
Conglomerate matrix support CM	Massive, m-thick bedded Syn-sedimentary	Poorly sorted pebbles supported in	Lithoclasts incl. shale clasts plus sand		None visible	Mass flow deposit. Associated with shale and turbidite sands in deep

	deformation structures	muddy matrix				subaqueous lacustrine setting
Conglomerate clast support CB	0.1 to 1m thick beds stacked up to 3 m units Erosive base, fining up	Well rounded pebbles in coarse sand-granule Clast support	Polymictic; Igneous, metamorphic and sedimentary rock pebbles in quartz, feldspar, lithoclast and mica coarse sand	Spar cement Locally with replaced & recrystallised shells	Interparticle	High energy event deposit Occurs adjacent to basin margin faults Alluvial fan or fan delta, where subaqueous
Modified Facies						
Chert CH	cm-0.2 m thick beds and as nodules Shrinkage cracks and fractured		Brown cryptocrystalline silica	Replacement of host sediments	None visible	Diagenetic replacement of marginal siliciclastic sands Possible palustrine silcretes
Breccia tectonic Bt	Fractured rocks With clay and sand filled fractures		Fractured host rocks	Spar cement in fractures	Fracture	Encountered in wells adjacent to basin bounding faults (e.g. Well 6)
Breccia karst Bk	Brecciated tops to beds	Clasts of host rock, reworked and set in fine sediment	Variable dependant on siliciclastic or carbonate host rock Iron oxides, calcite and silica nodules	Angular and coated grains Brecciation	Breccia	Brecciated tops of beds and associated mineralisation indicate emergent conditions

